At which magnetic field, exactly, does the Kondo resonance begin to split? A Fermi liquid description of the low-energy properties of the Anderson model

Michele Filippone,[1] Cătălin Paşcu Moca,[2,3] Jan von Delft,[4] and Christophe Mora[5]

[1]*Dahlem Center for Complex Quantum Systems and Institut für Theoretische Physik, Freie Universität Berlin, Arnimallee 14, 14195 Berlin, Germany*

[2]*BME-MTA Exotic Quantum Phase Group, Institute of Physics, Budapest University of Technology and Economics, H-1521 Budapest, Hungary*

[3]*Department of Physics, University of Oradea, 410087, Oradea, Romania*

[4]*Physics Department, Arnold Sommerfeld Center for Theoretical Physics and Center for NanoScience, Ludwig-Maximilians-Universität München, 80333 München, Germany*

[5]*Laboratoire Pierre Aigrain, École normale supérieure, PSL Research University, CNRS, Université Pierre et Marie Curie, Sorbonne Universités, Université Paris Diderot, Sorbonne Paris-Cit, 24 rue Lhomond, 75231 Paris Cedex 05, France*

(Received 22 September 2016; revised manuscript received 7 March 2017; published 5 April 2017)

We extend a recently developed Fermi liquid (FL) theory for the asymmetric single-impurity Anderson model [C. Mora *et al.*, Phys. Rev. B **92**, 075120 (2015)] to the case of an arbitrary local magnetic field. To describe the system's low-lying quasiparticle excitations for arbitrary values of the bare Hamiltonian's model parameters, we construct an effective low-energy FL Hamiltonian whose FL parameters are expressed in terms of the local level's spin-dependent ground-state occupations and their derivatives with respect to level energy and local magnetic field. These quantities are calculable with excellent accuracy from the Bethe ansatz solution of the Anderson model. Applying this effective model to a quantum dot in a nonequilibrium setting, we obtain exact results for the curvature of the spectral function, c_A, describing its leading $\sim \varepsilon^2$ term, and the transport coefficients c_V and c_T, describing the leading $\sim V^2$ and $\sim T^2$ terms in the nonlinear differential conductance. A sign change in c_A or c_V is indicative of a change from a local maximum to a local minimum in the spectral function or nonlinear conductance, respectively, as is expected to occur when an increasing magnetic field causes the Kondo resonance to split into two subpeaks. Surprisingly, we find that the fields B_A and B_V at which c_A and c_V change sign are parametrically different, with B_A of order T_K but B_V much larger. In fact, in the Kondo limit c_V never vanishes, implying that the conductance retains a (very weak) zero-bias maximum even for strong magnetic field and that the two pronounced finite-bias conductance side peaks caused by the Zeeman splitting of the local level do not emerge from zero-bias voltage.

DOI: 10.1103/PhysRevB.95.165404

I. INTRODUCTION

The Kondo effect, arising from the exchange interaction between a localized spin and delocalized conduction band, is characterized by a crossover between a fully screened singlet ground state and a free local spin at energies well above the Kondo temperature scale T_K. One of the most striking signatures of the Kondo effect is the occurrence of a sharp resonance near zero energy in the zero-temperature local spectral function $A(\varepsilon)$, which splits apart into two subresonances when a local magnetic field B is applied. Consequences of this Kondo peak and its field-induced splitting have been directly observed in numerous experimental studies of quantum dots tuned into the Kondo regime, where it causes a zero-bias peak in the nonlinear differential conductance $G(V)$, which splits into two subpeaks with increasing field. Indeed, the observation of a field-split zero-bias peak has come to be regarded as one of the hallmarks of the Kondo effect in the context of transport through quantum dots [1–7].

A minimal model for describing such experiments [8–11] is the two-lead, nonequilibrium, single-impurity Anderson model, describing a "dot" level with local interactions that hybridizes with two leads at different chemical potentials. Within the framework of this model (and its Kondo limit), numerous numerical and approximate analytical studies have explored the field-induced splitting of the Kondo peak in $A(\varepsilon)$ and of the zero-bias peak in $G(V)$ [12–28]. However, no *exact*, quantitative description exists for how these splittings come about [29]. For example, it is natural to expect that the emergence of split peaks is accompanied by a change of the curvatures $\partial_\varepsilon^2 A(\varepsilon)|_{\varepsilon=0}$ and $\partial_V^2 G(V)|_{V=0}$ from negative to positive [30]. A quantitative theory should yield exact results for the values of the "splitting fields," say B_A and B_V, respectively, at which these curvatures change sign. This information would be useful, for example, as benchmarks against which future numerical work on the nonequilibrium Anderson model could be tested.

In the present paper, we use Fermi liquid (FL) theory to compute these quantities exactly within the context of the two-lead, single-impurity Anderson model, for arbitrary particle-hole asymmetry. We develop an exact FL description of the low-energy regime where both the temperature T and the source-drain voltage V are much smaller than a crossover scale E_*, while the magnetic field B and the local level energy ε_d can be arbitrary. (In the local-moment regime at zero field, E_* corresponds to the Kondo temperature T_K). Though our theory does not capture the full shape of $A(\varepsilon)$ for arbitrary ε or $G(V)$ for arbitrary V, it does describe their curvatures at zero energy and voltage, respectively, for *arbitrary* values of B and ε_d.

Specifically, we compute two FL coefficients $\tilde{c}_A$ and c_A characterizing the zero-energy height and curvature of the spectral function, respectively, and two FL transport

 ©2017 American Physical Society

coefficients c_T and c_V characterizing the curvatures of the conductance as function of temperature T and bias voltage V, as well as the splitting fields B_A, B_T, and B_V at which c_A, c_T, and c_V vanish, respectively. In the Kondo limit in which the Anderson model maps onto the Kondo model, we find the universal ratios $B_A/T_K = 0.75073$ and $B_T/T_K = 1.54813$, where the Kondo temperature T_K is defined from the zero-field spin susceptibility.

More generally, we find that throughout the local-moment regime the splitting fields B_A and B_T are of order T_K, as expected from previous studies. Unexpectedly, however, the field B_V where the zero-bias conductance maximum changes into a minimum turns out to be much larger, namely $B_V \sim \sqrt{U\Delta}$, were U is the local Coulomb cost for double occupancy and Δ the local level width. Accordingly, B_V becomes infinitely large in the Kondo limit of $U/\Delta \to \infty$. Indeed, we show explicitly that in this limit c_V remains positive up to arbitrarily large fields. This unexpected result implies that the "natural" expectation expressed above, namely that the emergence of the two finite-bias peaks observed in $G(V)$ for $B \gtrsim T_K$ goes hand in hand with the emergence of a zero-bias minimum, is in fact incorrect: for the Kondo model, no zero-bias minimum ever appears in the conductance, regardless of field strength. However, the curvature of $G(V)$ around zero rapidly tends to zero with increasing field so that for practical purposes $G(V)$ looks completely flat at small voltages in large-field limit.

It should be stressed that the persistence of a very weak zero-bias maximum with increasing field does not contradict the emergence of two pronounced finite-bias maxima, which can be described analytically at large $V/T_K \gg 1$ [12,31]: these can coexist with the very weak local maximum at zero bias. It does show, however, that the two finite-bias peaks cannot emerge from zero bias but must appear at finite voltage (see Sec. III C). For the Anderson model, where c_V does turn negative at sufficiently large fields, our results imply that the two finite-bias conductance peaks appear long before the central zero-bias maximum has shrunk and flattened sufficiently to change into a minimum. We therefore conclude that in the field range $B \in [T_K, \sqrt{U\Delta}]$ the nonlinear conductance should actually exhibit three local maxima, with two pronounced side peaks emerging from the flanks of an increasingly weaker and flatter central maximum, with a very small curvature.

FL theories for quantum impurity systems have been originally introduced by Nozières [32] with phenomenological quasiparticles, and by Yamada and Yosida on a diagrammatic basis [33]. Later these theories were extended to orbital degenerate Anderson models [34–39], or extended in a renormalized perturbation theory [30,40–44]. They have also been extended to higher order terms in the low-energy perturbative expansion [45,46]. The FL approach used here to obtain the above results builds on a recent formulation by some of the present authors of a Fermi liquid theory for the single-impurity Anderson model [47], similar in spirit to the celebrated FL theory of Nozières for the Kondo model [32]. One useful feature of FL approaches [32,47–57] is that they provide exact results for the nonlinear conductance in out-of-equilibrium settings, albeit only in the limit that temperature and voltage are small compared to a characteristic FL energy scale E_*. For example, in Ref. [47], we obtained exact results for the differential conductance and the noise of the Anderson model for arbitrary particle-hole asymmetry [47], but zero magnetic field. The FL parameters of this effective theory were written in terms of ground-state properties which are computable semi-analytically using Bethe ansatz, or numerically via numerical renormalization group (NRG) calculations [58–60]. We here extend this FL approach to arbitrary magnetic fields. This enables us to obtain exact results for the low-energy behavior of the spectral function and the nonlinear conductance for any B and ε_d, and to explore the crossovers from the strong-coupling (screened-singlet) fixed point to the weak-coupling (free-spin) fixed point of the Anderson model as functions of both these parameters.

Our work is based on the fact that the Kondo ground state remains a Fermi liquid at finite magnetic field, as has been demonstrated by NRG in Ref. [61]. There the Korringa-Shiba relation on the spin susceptibility was shown to hold at arbitrary field, indicating that the low-energy excitations above the ground state are particle-hole pairs, as predicted by FL theory. Indeed, for both the Kondo and the Anderson models, there is a fundamental difference between a nonvanishing local magnetic field and other perturbations such as temperature or voltage. Electrons conserve their spin after scattering and are thus not sensitive to the chemical potential of the opposite spin species. At zero temperature and bias voltage, there is no room for inelastic processes, regardless of the value of the magnetic field, hence scattering remains purely elastic even when the Kondo singlet is destroyed due to the applied field. In contrast, increasing temperature or voltage open inelastic channels by deforming the Fermi surfaces of itinerant electrons.

The rest of the paper is organized as follows. Section II develops our FL theory for the asymmetric Anderson model at arbitrary local magnetic field and shows how the FL parameters can be expressed in terms of local spin and charge susceptibilities. In Sec. III, we exploit the effective FL Hamiltonian to evaluate the curvature parameters c_A, c_T, and c_V and the magnetic fields B_A, B_T, and B_V at which these curvatures change sign. This is done first at particle-hole symmetry, then for general particle-hole asymmetry. Our findings are summarized in Sec. IV.

II. FERMI LIQUID THEORY

A. Anderson model

The single-impurity Anderson model is a prototype model for magnetic impurities in bulk metals or for quantum dot nanodevices, and more generally for studying strong correlations in those systems. It describes an interacting spinful single level tunnel-coupled to a Fermi sea of itinerant electrons. Its Hamiltonian takes the form

$$H = \sum_{\sigma,k} \varepsilon_k c^\dagger_{k\sigma} c_{k\sigma} + \sum_\sigma \varepsilon_{d\sigma}\,\hat{n}_{d\sigma} + U\hat{n}_{d\uparrow}\hat{n}_{d\downarrow} + t\sum_{k,\sigma}(c^\dagger_{k\sigma} d_\sigma + d^\dagger_\sigma c_{k\sigma}). \tag{1}$$

Here, $d^\dagger_\sigma$ creates an electron with spin σ in a localized level with occupation number $\hat{n}_{d\sigma} = d^\dagger_\sigma d_\sigma$, spin-dependent energy $\varepsilon_{d\sigma} = \varepsilon_d - \sigma B/2$, local magnetic field B, and Coulomb penalty U for double occupancy. $c^\dagger_{k\sigma}$ creates an electron with spin σ

and energy ε_k in a conduction band with linear spectrum and constant density of states ν_0 per spin species. The local level and conduction band hybridize, yielding an escape rate $2\Delta = 2\pi\nu_0 t^2$.

We will denote the ground-state chemical potential for electrons of spin σ by $\mu_{0\sigma}$. Although $\mu_{0\uparrow}$ and $\mu_{0\downarrow}$ are usually taken equal, they formally are independent parameters that can be chosen to differ, because the model contains no spin-flip terms, hence spin-up and spin-down chemical potentials have no way to equilibrate. In this paper, we will consider only the limit of infinite bandwidth [62]. Then $\mu_{0\uparrow}$ and $\mu_{0\downarrow}$ constitute the only meaningful points of reference for the model's single-particle energy levels. Thus ground-state properties can depend on $\varepsilon_{d\sigma}$ and $\mu_{0\sigma}$ only in the combination $\varepsilon_{d\sigma} - \mu_{0\sigma}$, implying that they are invariant under shifts of the form

$$\varepsilon_{d\sigma} \to \varepsilon_{d\sigma} + \delta\mu_\sigma , \qquad \mu_{0\sigma} \to \mu_{0\sigma} + \delta\mu_\sigma . \tag{2}$$

In Ref. [47], this invariance was exploited for spin-independent shifts ($\delta\mu_\sigma = \delta\mu$) when devising a FL theory around the point $B = 0$. Here we will exploit the fact that the invariance holds also for spin-dependent shifts to generalize the FL theory to arbitrary B. Having made this point, we henceforth take $\mu_{0\uparrow} = \mu_{0\downarrow} = 0$ (but for clarity nevertheless display $\mu_{0\sigma}$ explicitly in some formulas). The model's zero-temperature, equilibrium properties are then fully characterized by U, Δ, ε_d, and B.

B. General strategy of FL theory à la Nozières

Despite exhibiting strong correlations by itself, the ground state of the Anderson model (1) is a Fermi liquid for all values of U, ε_d, Δ, and B. A corresponding FL theory à la Nozières was developed in [47] for small fields. We now briefly outline the general strategy used there, suitably adapted to accommodate arbitrary values of B. Details follow in subsequent sections.

The low-energy behavior of a quantum impurity model with a FL ground state can be understood in terms of weakly interacting quasiparticles, characterized by their energy ε, spin σ, distribution function $n_\sigma(\varepsilon)$, and the phase shift $\delta_\sigma(\varepsilon, n_{\sigma'})$ experienced upon scattering off the screened impurity. At zero temperature, the quasiparticle distribution reduces to a step function, $n^0_{\mu_{0\sigma}}(\varepsilon) = \theta(\mu_{0\sigma} - \varepsilon)$, and the phase shift at the chemical potential, denoted by $\delta_{0\sigma} = \delta_\sigma(\mu_{0\sigma}, n^0_{\mu_{0\sigma'}})$, is a characteristic property of the ground state. It is related to the impurity occupation function, $n_{d\sigma} = \langle \hat{n}_{d\sigma}\rangle$, via Friedel's sum rule, $\delta_{0\sigma} = \pi n_{d\sigma}$. Likewise, derivatives of $\delta_{0\sigma}$ with respect to (w.r.t.) ε_d and B are related to the ground-state values of the local charge and spin susceptibilities. The ground-state dependence of local observables such as $n_{d\sigma}$ and their derivatives on the model's bare parameters U, Δ, ε_d, and B is assumed to be known, e.g., from Bethe ansatz or numerics.

The goal of a FL theory is to use such ground-state information to predict the system's behavior at nonzero but low excitation energies. The weak residual interactions between low-energy quasiparticles can be treated perturbatively using a phenomenological effective Hamiltonian, $H_{\rm FL}$, whose form is fixed by general symmetry arguments. The coupling constants in $H_{\rm FL}$, together with $\delta_{0\sigma}$, are the "FL parameters" of the theory. The challenge is to express these in terms of ground-state properties, while ensuring that the theory remains invariant under the shifts of Eq. (2). To this end, $H_{\rm FL}$ is constructed in a way that is *independent* of $\mu_{0\sigma}$: it is expressed in terms of excitations relative to a *reference* ground state with distribution $n^0_{\varepsilon_{0\sigma}}$ and spin-dependent chemical potentials $\varepsilon_{0\sigma}$ chosen at some arbitrary values close to but not necessarily equal to $\mu_{0\sigma}$. The FL parameters are then functions of U, Δ, and the energy differences $\varepsilon_{d\sigma} - \varepsilon_{0\sigma}$. Importantly, and in keeping with their status of depending only on ground-state properties, they do not depend on the actual quasiparticle distribution functions n_σ, which are the only entities in the FL theory that depend on the actual chemical potential and temperature.

$H_{\rm FL}$ is used to calculate $\delta_\sigma(\varepsilon, n_{\sigma'})$ for a general quasiparticle distribution $n_{\sigma'}$, to lowest nontrivial order in the interactions. The result amounts to an expansion of the phase shift in powers of $\varepsilon - \varepsilon_{0\sigma}$ and $\delta n_\sigma = n_\sigma - n^0_{\varepsilon_{0\sigma}}$, which are assumed small. Since the reference energies $\varepsilon_{0\sigma}$ are dummy variables on which no physical observables should depend, this expansion must be *independent* of $\varepsilon_{0\sigma}$. This requirement leads to a set of so-called "Fermi liquid relations" between the FL parameters, which can be used to express them all in terms of various local ground-state observables, thereby completing the specification of $H_{\rm FL}$. Finally, $H_{\rm FL}$ is used to calculate transport properties at low temperature and voltage.

C. Low-energy effective model

The phenomenological FL Hamiltonian has the form

$$H_{\rm FL} = \sum_\sigma \int_\varepsilon \varepsilon\, b^\dagger_{\varepsilon\sigma} b_{\varepsilon\sigma} + H_\alpha + H_\phi + \dots \tag{3a}$$

$$H_\alpha = -\sum_\sigma \int_{\varepsilon_1,\varepsilon_2} \left[\frac{\alpha_{1\sigma}}{2\pi}(\varepsilon_1 + \varepsilon_2 - 2\varepsilon_{0\sigma}) + \frac{\alpha_{2\sigma}}{4\pi}(\varepsilon_1 + \varepsilon_2 - 2\varepsilon_{0\sigma})^2 \right] b^\dagger_{\varepsilon_1\sigma} b_{\varepsilon_2\sigma} , \tag{3b}$$

$$H_\phi = \int_{\varepsilon_1,\dots,\varepsilon_4} \left[\frac{\phi_1}{\pi} + \frac{\phi_{2\uparrow}}{4\pi}(\varepsilon_1 + \varepsilon_2 - 2\varepsilon_{0\uparrow}) + \frac{\phi_{2\downarrow}}{4\pi}(\varepsilon_3 + \varepsilon_4 - 2\varepsilon_{0\downarrow}) \right] : b^\dagger_{\varepsilon_1\uparrow} b_{\varepsilon_2\uparrow} b^\dagger_{\varepsilon_3\downarrow} b_{\varepsilon_4\downarrow} : . \tag{3c}$$

It is a perturbative low-energy expansion involving excitations with respect to a reference ground state with chemical potentials $\varepsilon_{0\sigma}$ and distribution function $n^0_{\varepsilon_{0\sigma}}(\varepsilon) = \theta(\varepsilon_{0\sigma} - \varepsilon)$. The dummy reference energies $\varepsilon_{0\sigma}$ should be chosen close to $\mu_{0\sigma}$ for this expansion to make sense. Here, $b^\dagger_{\varepsilon\sigma}$ creates a quasiparticle in a scattering state with spin σ and excitation energy $\varepsilon - \varepsilon_{0\sigma}$ relative to the reference state; it already incorporates the zero-temperature phase shift $\delta_{0\sigma}$. Moreover, : : denotes normal ordering w.r.t. the reference state, with

$$: b^\dagger_{\varepsilon\sigma} b_{\varepsilon\sigma} : \equiv b^\dagger_{\varepsilon\sigma} b_{\varepsilon\sigma} - n^0_{\varepsilon_{0\sigma}}(\varepsilon) . \tag{4}$$

H_α and H_ϕ describe elastic and inelastic scattering processes, respectively. Their formal structure can be justified using conformal field theory and symmetry arguments [45,63,64], summarized in Supplementary section S-IV of Ref. [47]. They contain the leading and subleading terms in a classification of all possible perturbations according to their scaling dimensions, which characterize their importance at low excitation energies with respect to the reference state. The coupling constants in $H_{\rm FL}$, together with the zero-energy phase shifts $\delta_{0\sigma}$, are the model's nine FL parameters, which we will generically denote by $\gamma \in \{\delta_{0\sigma},\alpha_{1\sigma},\alpha_{2\sigma},\phi_1,\phi_{2\sigma}\}$.

In the wide-band limit considered here, all FL parameters depend on the model parameters only in the form

$$\gamma = \gamma(U,\Delta,\varepsilon_{d\sigma}-\varepsilon_{0\sigma}), \tag{5}$$

because the chemical potential $\varepsilon_{0\sigma}$ of our reference ground state is the only possible point of reference for the local energies $\varepsilon_{d\sigma}$. Writing $\varepsilon_{0\sigma}=\varepsilon_0-\sigma B_0/2$, we thus note that all FL parameters satisfy the relations

$$-\partial_{\varepsilon_0}\gamma = \partial_{\varepsilon_d}\gamma\,, \quad -\partial_{B_0}\gamma = \partial_B\gamma\,. \tag{6}$$

The form of $H_{\rm FL}$ in Eq. (3) is similar to that used in Ref. [47], but with two changes, both due to considering $B\neq 0$. First, because the magnetic field breaks spin symmetry, some FL coefficients are now spin dependent, namely, those that occur in conjunction with excitation energies of the form $(\varepsilon-\varepsilon_{0\sigma})$. Second, since the FL theory of Ref. [47] was developed around the point $B=0$, the FL parameters there were taken to be independent of field, and the system's response to a small field was studied by explicitly including a small Zeeman term in $H_{\rm FL}$. In contrast, in the present formulation the FL parameters are functions of B that explicitly incorporate the full magnetic-field dependence of all ground-state properties, hence our $H_{\rm FL}$ does not need an explicit Zeeman term.

To conclude this section, we note that the form of $H_{\rm FL}$ presented above can be derived by an explicit calculation in a particular limiting case: the Kondo limit of the Anderson Hamiltonian where it can be mapped onto the Kondo Hamiltonian, studied in the limit of very large magnetic field. By doing perturbation theory in the spin-flip terms of the Kondo Hamiltonian, one arrives at effective interaction terms that have precisely the form of H_α and H_ϕ above. This calculation, presented in detail in Appendix A, is highly instructive, because it elucidates very clearly how the reference energies $\varepsilon_{0\sigma}$ enter the analysis and how the relations (5) and (6) come about.

D. Relating FL parameters to local observables

Having presented the general form of $H_{\rm FL}$, the next step is to express the FL parameters in terms of ground-state observables. The corresponding relations are conveniently derived by examining the elastic phase shift of a single quasiparticle excitation [54]. We suppose that the system is in an arbitrary state, not too far from the ground state, characterized by the spin-dependent number distribution $\langle b^\dagger_{\varepsilon\sigma}b_{\varepsilon'\sigma}\rangle = n_\sigma(\varepsilon)\delta(\varepsilon-\varepsilon')$, with arbitrary $n_\sigma(\varepsilon)$. The elastic phase shift of a quasiparticle with energy ε and spin σ scattered off this state is obtained from the elastic part H_α, in addition to the Hartree diagrams inherited from H_ϕ, thus $\delta_\sigma(\varepsilon,n_{\sigma'}) = \delta_{0\sigma}-\pi\partial\langle H_\alpha+H_\phi\rangle/\partial_{n_\sigma(\varepsilon)}$. One finds the expansion

$$\begin{aligned}\delta_\sigma(\varepsilon,n_{\sigma'}) &= \delta_{0\sigma}+\alpha_{1\sigma}(\varepsilon-\varepsilon_{0\sigma})+\alpha_{2\sigma}(\varepsilon-\varepsilon_{0\sigma})^2\\ &\quad -\int_{\varepsilon'}\left[\phi_1+\frac{1}{2}\phi_{2\sigma}(\varepsilon-\varepsilon_{0\sigma})+\frac{1}{2}\phi_{2\bar\sigma}(\varepsilon'-\varepsilon_{0\bar\sigma})\right]\\ &\quad\times\delta n_{\bar\sigma}(\varepsilon').\end{aligned} \tag{7}$$

Due to the normal ordering prescription for H_ϕ, all terms stemming from the latter involve the difference between the actual and reference distribution functions, $\delta n_{\bar\sigma}=n_{\bar\sigma}-n^0_{\varepsilon_{0\bar\sigma}}$, where $\bar\sigma$ denotes the spin opposite to σ. Now, though expansion (7) depends on $\varepsilon_{0\sigma}$ both explicitly and via the FL parameters $\gamma(U,\Delta,\varepsilon_{d\sigma}-\varepsilon_{0\sigma})$, these dependencies have to conspire in such a way that the phase shift is actually *independent* of $\varepsilon_{0\sigma}$. Thus the following conditions must be satisfied:

$$\partial_{\varepsilon_0}\delta_\sigma(\varepsilon,n_{\sigma'})=0, \qquad \partial_{B_0}\delta_\sigma(\varepsilon,n_{\sigma'})=0. \tag{8}$$

Inserting Eq. (7), setting the coefficients of the various terms in the expansion (const., $\sim(\varepsilon-\varepsilon_{0\sigma})$, $\propto\int\delta n_{\bar\sigma}$) to zero and exploiting Eq. (6), we obtain a set of linear relations among the FL parameters, to be called "Fermi liquid relations:"

$$\frac{\partial\delta_{0\sigma}}{\partial\varepsilon_d}=\phi_1-\alpha_{1\sigma}, \quad \frac{\partial\delta_{0\sigma}}{\partial B}=\frac{\sigma}{2}(\phi_1+\alpha_{1\sigma}), \tag{9a}$$

$$\frac{\partial\alpha_{1\sigma}}{\partial\varepsilon_d}=\frac{1}{2}\phi_{2\sigma}-2\alpha_{2\sigma}, \quad \frac{\partial\alpha_{1\sigma}}{\partial B}=\frac{\sigma}{2}\left(\frac{1}{2}\phi_{2\sigma}+2\alpha_{2\sigma}\right), \tag{9b}$$

$$\frac{\partial\phi_1}{\partial\varepsilon_d}=-\frac{1}{2}(\phi_{2\uparrow}+\phi_{2\downarrow}), \quad \frac{\partial\phi_1}{\partial B}=\frac{1}{4}(\phi_{2\uparrow}-\phi_{2\downarrow}). \tag{9c}$$

They are important for three reasons. First, for fixed values of the model parameters, they ensure by construction that $\delta_\sigma(\varepsilon,n_{\sigma'})$ is invariant under spin-dependent shifts of the dummy reference energies $\varepsilon_{0\sigma}$. Second, for fixed values of $\varepsilon_{0\sigma}$, they ensure that for any distribution $n_{\sigma'}$ with well-defined chemical potentials $\mu_{\sigma'}$, the function $\delta_\sigma(\varepsilon,n_{\sigma'})$ is invariant, up to a shift in ε, under simultaneous spin-dependent shifts [cf. Eq. (2)] of the physical model parameters $\varepsilon_{d\sigma'}$ and $\mu_{\sigma'}$, say by $\delta\mu_{\sigma'}=\delta\mu-\frac{1}{2}\sigma'h$:

$$\delta_\sigma(\varepsilon+\delta\mu_\sigma,n_{\sigma'})|_{\varepsilon_{d\sigma'}+\delta\mu_{\sigma'},\mu_{\sigma'}+\delta\mu_{\sigma'}}=\delta_\sigma(\varepsilon,n_{\sigma'})|_{\varepsilon_{d\sigma'},\mu_{\sigma'}}. \tag{10}$$

Conversely, an alternative way to derive Eq. (9) is to impose Eq. (10) as a condition on the expansion (7). (Verifying this is particularly simple at zero temperature, e.g., using $n_{\sigma'}=n^0_{\mu_{0\sigma}}$). In the parlance of Nozières [32], Eq. (10) is the "strong universality" version of his "floating Kondo resonance" argument, applied to the Anderson model. Pictorially speaking, for each spin species the phase shift function "floats" on the Fermi sea of corresponding spin: if the Fermi surface μ_σ and local level $\varepsilon_{d\sigma}$ for spin σ are both shifted by $\delta\mu_\sigma$, the phase shift function $\delta_\sigma(\varepsilon,n_{\sigma'})$ shifts along without changing its shape.

Third, the Fermi liquid relations, in conjunction with Friedel's sum rule, can be used to link the FL parameters to ground-state values of local observables. To this end, we henceforth set $\varepsilon_{0\sigma}=\mu_{0\sigma}$ and focus on the case of zero temperature with ground-state distribution $n^0_{\mu_{0\sigma}}$. Then only the first term in Eq. (7) survives when writing down Friedel's sum rule for the phase shift at the chemical potential:

$$\delta_\sigma\left(\mu_{0\sigma},n^0_{\mu_{0\sigma'}}\right)=\delta_{0\sigma}=\pi n_{d\sigma}\,. \tag{11}$$

Let $n_d = \sum_\sigma n_{d\sigma}$ and $m_d = \frac{1}{2}\sum_\sigma \sigma n_{d\sigma}$ denote the average local charge and magnetization, respectively, and let us introduce corresponding even and odd linear combinations of the spin-dependent FL parameters, to be denoted without or with overbars, e.g., $\alpha_1 = \frac{1}{2}\sum_\sigma \alpha_{1\sigma}$ and $\overline{\alpha}_1 = \frac{1}{2}\sum_\sigma \sigma\alpha_{1\sigma}$. Then we have $n_d = 2\delta_0/\pi$ and $m_d = \overline{\delta}_0/\pi$. By differentiating these relations with respect to ε_d and B, we obtain various local susceptibilities, which can be expressed, via the derivates occurring in Eq. (9), as linear combinations of FL parameters:

$$\chi_c = -\frac{\partial n_d}{\partial \varepsilon_d} = \frac{2}{\pi}(\alpha_1 - \phi_1), \tag{12a}$$

$$\chi_s = \frac{\partial m_d}{\partial B} = \frac{1}{2\pi}(\alpha_1 + \phi_1), \tag{12b}$$

$$\chi_m = -\frac{\partial m_d}{\partial \varepsilon_d} = \frac{\partial n_d}{\partial B} = \frac{\overline{\alpha}_1}{\pi}, \tag{12c}$$

$$\frac{\partial \chi_c}{\partial \varepsilon_d} = -\frac{\partial^2 n_d}{\partial {\varepsilon_d}^2} = -\frac{4}{\pi}\left(\alpha_2 - \frac{3}{4}\phi_2\right), \tag{12d}$$

$$\frac{\partial \chi_s}{\partial B} = \frac{\partial^2 m_d}{\partial B^2} = \frac{1}{2\pi}\left(\overline{\alpha}_2 + \frac{3}{4}\overline{\phi}_2\right), \tag{12e}$$

$$\frac{\partial \chi_m}{\partial \varepsilon_d} = -\frac{\partial^2 m_d}{\partial {\varepsilon_d}^2} = \frac{\partial^2 n_d}{\partial B \partial \varepsilon_d} = -\frac{2}{\pi}\left(\overline{\alpha}_2 - \frac{\overline{\phi}_2}{4}\right), \tag{12f}$$

$$\frac{\partial \chi_m}{\partial B} = \frac{\partial^2 n_d}{\partial B^2} = -\frac{\partial^2 m_d}{\partial \varepsilon_d \partial B} = \frac{1}{\pi}\left(\alpha_2 + \frac{\phi_2}{4}\right). \tag{12g}$$

Equation (12c) reproduces a standard thermodynamic identity, and implies similar identities for higher derivates, $\partial\chi_m/\partial\varepsilon_d = -\partial\chi_c/\partial B$ and $\partial\chi_m/\partial B = -\partial\chi_s/\partial\varepsilon_d$. By inverting the above relations, we obtain the FL parameters in terms of local ground-state susceptibilities:

$$\frac{\alpha_1}{\pi} = \chi_s + \frac{1}{4}\chi_c, \quad \frac{\alpha_2}{\pi} = \frac{3}{4}\frac{\partial \chi_m}{\partial B} - \frac{1}{16}\frac{\partial \chi_c}{\partial \varepsilon_d}, \tag{13a}$$

$$\frac{\phi_1}{\pi} = \chi_s - \frac{1}{4}\chi_c, \quad \frac{\phi_2}{\pi} = \frac{\partial \chi_m}{\partial B} + \frac{1}{4}\frac{\partial \chi_c}{\partial \varepsilon_d}, \tag{13b}$$

$$\frac{\overline{\alpha}_1}{\pi} = \chi_m, \quad \frac{\overline{\alpha}_2}{\pi} = \frac{1}{2}\frac{\partial \chi_s}{\partial B} - \frac{3}{8}\frac{\partial \chi_m}{\partial \varepsilon_d}, \tag{13c}$$

$$\frac{\overline{\phi}_2}{\pi} = 2\frac{\partial \chi_s}{\partial B} + \frac{1}{2}\frac{\partial \chi_m}{\partial \varepsilon_d}, \tag{13d}$$

implying that $\phi_2 = -\partial_{\varepsilon_d}\phi_1$ and $\overline{\phi}_2 = 2\partial_B\phi_1$. These equations are a central technical result of this paper. Those for the even FL parameters $\alpha_{1,2}$ and $\phi_{1,2}$ are equivalent to the ones obtained, for zero field, in Ref. [47]. The expressions for α_1 and ϕ_1 have been shown [47] to be equivalent to the relation

$$\frac{4\chi_s}{(g\mu_B)^2} + \chi_c = \frac{6\gamma_{\mathrm{imp}}}{\pi^2 k_B^2}, \tag{14}$$

(physical units have been reinstated in this equation) between the spin/charge susceptibilities and the impurity specific heat coefficient γ_{imp} [42]. This relation in fact derives from Ward identities [33,34] associated with the U(1) symmetry of the model. We expect that the other expressions in Eq. (13) also originate from Ward identities involving higher-order derivatives.

Equations (13) can be checked independently in two limits: for a noninteracting impurity, and at large magnetic field in the Kondo model, see Appendix A for the latter. The former case, $U = 0$, reduces to a resonant level model in which spin and charge susceptibilities are easily obtained. We have verified that they give $\phi_1 = \phi_{2\sigma} = 0$, so that the interaction $H_\phi = 0$ in Eq. (3) vanishes, and that the phase shift expansion (7) reproduces that expected for the resonant level model.

All of the susceptibilities introduced above are calculable exactly by Bethe ansatz, and hence the same is true for all the FL parameters. In the particle-hole symmetric case, $\varepsilon_d = -U/2$, semianalytical expressions for the local charge and magnetization have been derived with the help of the Wiener-Hopf method. A comprehensive review on this approach can be found in Ref. [64] and we summarize the resulting analytical expressions in Ref. [65]. They have been used to produce Figs. 1 to 4 below with excellent accuracy.

Away from particle-hole symmetry, where the Wiener-Hopf method is not applicable, the Bethe ansatz coupled integral equations (see Eqs. (S3a) and (S3b) in the Supplemental Material [65]) have to be solved numerically. This direct method is used in Figs. 6 and 7. In Fig. 4, we have verified that at particle-hole symmetry it agrees nicely with the accurate Wiener-Hopf solution.

To conclude this section, we briefly discuss some special cases, for future reference. (i) *Zero magnetic field.* Equations (13) for the odd FL parameters yield zero for $B = 0$,

$$\overline{\alpha}_1 = \overline{\alpha}_2 = \overline{\phi}_2 = 0, \tag{15}$$

since m_d is an antisymmetric function of B.

(ii) *Particle-hole symmetry.* At $\varepsilon_d = -U/2$, we have

$$n_d = 1, \;\; \delta_{0\sigma} = \pi\left(\tfrac{1}{2} + \sigma m_d\right), \;\; \overline{\alpha}_1 = \alpha_2 = \phi_2 = 0, \tag{16}$$

for any B. The three FL parameters vanish since $n_d - 1$ is an antisymmetric function of $\varepsilon_d - U/2$, implying the same for χ_m and $\partial\chi_c/\partial\varepsilon_d$, so that both vanish at $\varepsilon_d = -U/2$.

(iii) *Kondo limit.* If the limit $U/\Delta \to \infty$ is taken at particle-hole symmetry while maintaining a finite Kondo temperature, local charge fluctuations are frozen out completely and the Anderson model maps onto the Kondo model. All susceptibilities involving derivatives of n_d with respect to ε_d vanish, namely $\chi_c = \chi_m = \partial_{\varepsilon_d}\chi_c = \partial_{\varepsilon_d}\chi_s = \partial_B\chi_c = 0$, so that Eq. (16) are supplemented by

$$\frac{\alpha_1}{\pi} = \frac{\phi_1}{\pi} = \chi_s, \qquad \frac{4\overline{\alpha}_2}{\pi} = \frac{\overline{\phi}_2}{\pi} = 2\frac{\partial \chi_s}{\partial B}. \tag{17}$$

Since χ_s and $\partial\chi_s/\partial B$ are strictly positive and negative, respectively, the same is true for α_1, ϕ_1 and $\overline{\alpha}_2, \overline{\phi}_2$.

(iv) *Kondo limit at large fields.* In the limit $B \gg T_K$ of the Kondo model, its Bethe ansatz solution yields the following results for the leading asymptotic behavior of the magnetization and its derivatives, with $\beta_r = \frac{\pi}{8}(B/T_K)^2$:

$$m_d = \frac{1}{2} - \frac{1}{2\ln\beta_r}, \quad \chi_s = \frac{1}{B\,(\ln\beta_r)^2}, \tag{18a}$$

$$\frac{\partial\chi_s}{\partial B} = -\frac{1}{B^2\,(\ln\beta_r)^2}. \tag{18b}$$

Thus all the FL parameters in Eq. (17) vanish asymptotically in the large-field limit.

E. Characteristic FL energy scale

As mentioned repeatedly above, the FL approach only holds for excitation energies sufficiently small, say $|\varepsilon - \mu_{0\sigma}| \ll E_*$, that all terms in expansion (7) for $\delta_\sigma(\varepsilon, n_{\sigma'}) - \delta_{0\sigma}$ are small. In the local moment regime of the Anderson model, the FL scale E_* can be associated with the Kondo temperature T_K, but in the present context we need a definition applicable in the full parameter space of the Anderson model. Following Ref. [47], we define E_* in terms of the FL coefficient of the leading term in expansion (7),

$$E_* = \frac{\pi}{4\alpha_1} = \frac{1}{4\chi_s + \chi_c}\,, \tag{19}$$

and T_K in terms of the zero-field spin susceptibility,

$$T_K = \frac{1}{4\chi_s^{B=0}}\,. \tag{20}$$

While both definitions involve some arbitrariness, they are mutually consistent, in that the zero-field value of E_* equals T_K in the Kondo limit $U/\Delta \to \infty$, where we have

$$E_*^{B=0} = T_K, \qquad E_*^{B\gg T_K} = \tfrac{1}{4}B(\ln \beta_r)^2\,. \tag{21}$$

More generally, $E_*^{B=0}$ and T_K are roughly equal throughout the local-moment regime where $\chi_c \simeq 0$, i.e., for $U \gg \Delta$ and $-U + \Delta \lesssim \varepsilon_d \lesssim -\Delta$. In this regime, T_K is well described by the analytic formula (af) [47,66,67]

$$T_K^{(\mathrm{af})} = \sqrt{\tfrac{U\Delta}{2}}\, e^{\pi\left(\frac{\Delta}{2U} - \frac{U}{8\Delta}\right)} e^{x^2}\,, \tag{22}$$

where $x = (\varepsilon_d + U/2)\sqrt{\pi/(2\Delta U)}$ measures the distance to the particle-hole symmetric point. At the latter, $T_K^{(\mathrm{af})}|_{x=0}$ can be derived analytically from the Bethe ansatz equations for $\chi_s^{B=0}$ [64]. The factor e^{x^2}, familiar from Haldane's RG treatment of the Anderson model [66], phenomenologically includes the effect of particle-hole asymmetry. Throughout the local moment regime, Eq. (22) yields excellent agreement with a direct numerical evaluation of Eq. (20) via the Bethe ansatz equations for $\chi_s^{B=0}$ (see Fig. 6 below).

III. SPECTRAL FUNCTION AND NONLINEAR CONDUCTANCE

A. General results

For the remainder of this paper, we consider a single-level quantum dot with symmetric tunnel couplings to left and right leads with chemical potentials $\pm eV/2$, described by the two-lead, single-level Anderson model. The nonlinear conductance of this system can be expressed by the Meir-Wingreen formula as [68]

$$G(V,T) = \partial_V \frac{e}{h} \int_\varepsilon [f_L(\varepsilon) - f_R(\varepsilon)] A(\varepsilon)\,. \tag{23}$$

Here, $f_{L/R}(\varepsilon) = [e^{(\varepsilon \mp eV/2)/T} + 1]^{-1}$ are the distribution functions of the left and right leads, $A(\varepsilon) = \sum_\sigma A_\sigma(\varepsilon)$ is the local spectral function with spin components $A_\sigma(\varepsilon) = -\pi\nu_0\, \mathrm{Im}\mathcal{T}_\sigma(\varepsilon)$, and $\mathcal{T}_\sigma(\varepsilon)$ is the T matrix for spin σ conduction electrons scattering off the local level. A FL calculation of the low-energy behavior of $A_\sigma(\varepsilon)$ and $G(V,T)$ has been performed in detail at zero magnetic field in Ref. [47], following similar studies in Refs. [38,53,55,56]. The strategy of the calculation is rather straightforward. First, one introduces even and odd linear combinations of operators from the two leads. The odd ones decouple, resulting in an effective one-lead Anderson model for a dot coupled to the even lead, whose low-energy behavior is described by the Hamiltonian H_{FL} introduced above. Then, in the spirit of the standard Landauer-Büttiker formalism [69], the current operator is expanded over a convenient single-particle basis of scattering states accounting for both the lead-dot geometry and the FL elastic phase shifts. Interactions between electrons stemming from H_ϕ are included perturbatively when calculating the average current in the Keldysh formalism [70].

The calculation described above trivially generalizes to the case of nonzero field, since the two spin components give separate contributions to the current. The results from Ref. [47] for the low-energy expansion of the conductance can thus be directly taken over, modified merely by supplying FL parameters with spin indices. A corresponding low-energy expansion for the spectral function can then be deduced via Eq. (23). We now present the results obtained in this manner, starting with the T matrix and spectral function, since these form the basis for understanding the resulting physical behavior.

For the T matrix, written as the sum of elastic and inelastic contributions, the results of Ref. [47] (Supplementary section S-V) imply

$$\mathcal{T}_\sigma^{\mathrm{el}}(\varepsilon) = -\frac{i}{2\pi\nu_0}\left(1 - e^{2i\delta_\sigma(\varepsilon)}\right), \tag{24a}$$

$$\mathcal{T}_\sigma^{\mathrm{inel}}(\varepsilon) = -\frac{i e^{2i\delta_{0\sigma}}}{2\pi\nu_0}\phi_1^2\left[\varepsilon^2 + (\pi T)^2 + \frac{3}{4}(eV)^2\right]. \tag{24b}$$

Here, $\mathcal{T}_\sigma^{\mathrm{el}}(\varepsilon)$ is determined by the phase shift $\delta_\sigma(\varepsilon)$ obtained from Eq. (7) using $n_\sigma(\varepsilon) = \frac{1}{2}[f_L(\varepsilon) + f_R(\varepsilon)]$ as quasiparticle distribution function for the even lead:

$$\delta_\sigma(\varepsilon) = \delta_{0\sigma} + \alpha_{1\sigma}\varepsilon + \alpha_{2\sigma}\varepsilon^2 - \tfrac{1}{12}\phi_{2\sigma}\left[(\pi T)^2 + \tfrac{3}{4}(eV)^2\right]. \tag{25}$$

Note that the inelastic T matrix has the same dependence on temperature and bias, which occur only in the combination $(\pi T)^2 + \frac{3}{4}(eV)^2$ [71].

This is significant, since it implies that knowing the spectral function's leading temperature dependence in *equilibrium* suffices to deduce its leading bias dependence in nonequilibrium. The spectral function, expanded to second order in ε, T, and eV, can thus be written as [72]

$$A(\varepsilon) = A_0 + A_1\varepsilon - \widetilde{C}_A\left[\tfrac{1}{3}(\pi T)^2 + \tfrac{1}{4}(eV)^2\right] - C_A\varepsilon^2, \tag{26}$$

with expansion coefficients

$$A_0 = \sum_\sigma \sin^2(\delta_{0\sigma}), \quad A_1 = \sum_\sigma \alpha_{1\sigma}\sin(2\delta_{0\sigma}), \tag{27a}$$

$$\widetilde{C}_A = -\sum_\sigma \left[\frac{3}{2}\phi_1^2\cos(2\delta_{0\sigma}) - \frac{1}{4}\phi_{2\sigma}\sin(2\delta_{0\sigma})\right], \tag{27b}$$

$$C_A = -\sum_\sigma \left[<\left(\alpha_{1\sigma}^2 + \frac{1}{2}\phi_1^2\right)\cos(2\delta_{0\sigma}) + \alpha_{2\sigma}\sin(2\delta_{0\sigma})\right]. \tag{27c}$$

These results hold for all values of U, Δ, ε_d, and B.

Inserting Eq. (26) into (23) and using the relations

$$\partial_V \int_\varepsilon [f_L - f_R]\varepsilon^2 = e\left[\frac{1}{3}(\pi T)^2 + \frac{1}{4}(eV)^2\right],$$
$$\partial_V \int_\varepsilon [f_L - f_R]\left[\frac{1}{3}(\pi T)^2 + \frac{1}{4}(eV)^2\right]$$
$$= e\left[\frac{1}{3}(\pi T)^2 + \frac{3}{4}(eV)^2\right], \tag{28}$$

one obtains an expansion for the conductance of the form

$$G(V,T) = \widetilde{G} - (2e^2/h)[C_T T^2 + C_V (eV)^2]. \tag{29}$$

Here, $\widetilde{G} = \frac{1}{2}A_0 G_0$ is the zero-temperature, linear conductance, $G_0 = 2e^2/h$ is the conductance quantum, and the expansion coefficients of the quadratic terms are

$$C_T = \tfrac{1}{6}\pi^2(\widetilde{C}_A + C_A), \quad C_V = \tfrac{1}{8}(3\widetilde{C}_A + C_A). \tag{30}$$

The four C coefficients introduced above all have dimensions of (energy)$^{-2}$. If we express them as

$$\widetilde{C}_A = \frac{\tilde{c}_A}{E_*^2}, \quad C_X = \frac{c_X}{E_*^2}, \quad X = A, V, T, \tag{31}$$

where E_* is the FL scale of Eq. (19), the resulting four c coefficients are dimensionless, with c_T and c_V corresponding to the coefficients calculated in Ref. [47]. For asymmetric couplings to the leads [73–75], not considered here, the conductance also contains a term linear in V, as also discussed in Ref. [55], where the same formalism has been applied.

Equations (27) instructively reveal which role the various FL parameters play in determining the shape of the local spectral function $A(\varepsilon)$ at the chemical potential, characterized by its "height" $A(0)$, slope A_1 and curvature $\widetilde{C}_A$. The ground-state phase shifts $\delta_{0\sigma}$ fix the height at zero temperature and bias, A_0. The elastic couplings $\alpha_{1\sigma}$ and $\alpha_{2\sigma}$ of H_α affect only the slope and curvature, but not the height. The inelastic couplings ϕ_1 and $\phi_{2\sigma}$ of H_ϕ determine the leading effect of temperature and bias on the height via $\widetilde{C}_A$, while ϕ_1 also contributes to the curvature C_A. Moreover, via the sine and cosine factors the relative contributions of all terms depend sensitively on the ground-state phase shifts $\delta_{0\sigma}$, and hence can change significantly when these are tuned via changing parameters such as B or ε_d.

B. Spectral function at particle-hole symmetry

When the single-level, two-lead Anderson model is tuned into the local moment regime, the local spectral function exhibits a Kondo peak that splits with magnetic field. Correspondingly, the nonlinear conductance exhibits a zero-bias peak that likewise splits with increasing field. Our goal is to use FL theory to study the peak splittings of both the spectral function and the nonlinear conductance in quantitative detail. For this purpose, we will focus on the particle-hole symmetric point in this subsection and the next, leaving particle-hole asymmetry to Sec. III D.

We begin with a qualitative discussion, based on the results of numerous previous studies of the local moment regime [12,31,49,76–80]. At zero field, the two components of the local spectral function, $A_\uparrow$ and $A_\downarrow$, both exhibit a Kondo peak at zero energy. An increasing field weakens these peaks and shifts them in opposite directions. When their splitting exceeds their width, which happens for B of order T_K, then $A = A_\uparrow + A_\downarrow$ develops a local minimum at zero energy, implying that C_A changes from positive to negative. We will denote the "splitting field" where $C_A = 0$ by B_A. [For $B \gg T_K$ the subpeaks in $A_{\uparrow,\downarrow}$ are located at $\varepsilon \simeq \pm B$, modulo corrections of order $\mp B/\ln(B/T_K)$ [12,79,80]]. An increasing temperature or bias always weakens the Kondo peaks in A_σ, thus reducing the zero-energy spectral height $A(0)$ ("height reduction"), so that we expect $\widetilde{C}_A$ to be a decreasing but strictly positive function of B.

To study this behavior quantitatively, we specialize the results of the previous section to the case of particle-hole symmetry using Eq. (16), obtaining

$$A_0 = 2\cos^2(\pi m_d), \tag{32a}$$
$$\widetilde{C}_A = 3\phi_1^2 \cos(2\pi m_d) - \tfrac{1}{2}\overline{\phi}_2 \sin(2\pi m_d), \tag{32b}$$
$$C_A = \left(2\alpha_1^2 + \phi_1^2\right)\cos(2\pi m_d) + 2\overline{\alpha}_2 \sin(2\pi m_d). \tag{32c}$$

Figure 1 shows the B dependence of $\tilde{c}_A = E_*^2\widetilde{C}_A$ and $c_A = E_*^2 C_A$ for several values of U/Δ. (We multiply by the B-dependent scale E_*^2 [cf. Eq. (31)], since this better reveals the large-field behavior, for reasons explained below). For comparison, we have also used NRG [81] to compute the equilibrium spectral function (not shown) for the Anderson model at finite magnetic field. The $\widetilde{C}_A$ and C_A values obtained by fitting its zero-energy height and curvature, shown as open circles in the inset of Figs. 1(a) and 1(b), respectively, agree very well with our FL predictions (solid lines). This serves as independent confirmation that our FL theory is sound.

The main finding of Fig. 1 is that with increasing field, $\tilde{c}_A$ remains positive, whereas c_A changes sign, as expected from our qualitative discussion. Thus our FL approach reproduces the field-induced splitting of the Kondo peak in the spectral function. Moreover, we find [Fig. 1(c)] that the scale for the splitting field B_A is *universal*, in the usual sense familiar from many aspects of Kondo physics in the Anderson model: the ratio B_A/T_K is of order unity and depends only weakly on U/Δ, tending to a constant value in the Kondo limit $U/\Delta \to \infty$. Its limiting value, namely $B_A/T_K = 0.75073$, agrees with previous numerical estimates [76,77] and with our own NRG calculation.

Perhaps somewhat less expected is the fact that the large-field behavior of $\tilde{c}_A$ and c_A changes significantly with increasing U/Δ. To understand their behavior in the Kondo limit $U/\Delta \to \infty$, we first consider that of $\widetilde{C}_A$ and C_A, for which Eqs. (32) and (17) yield

$$\begin{Bmatrix} \widetilde{C}_A \\ C_A \end{Bmatrix} = 3\alpha_1^2 \cos(2\pi m_d) \mp 2\overline{\alpha}_2 \sin(2\pi m_d), \tag{33}$$

with zero-field values (indicated by a superscript K for "fully developed Kondo effect") of

$$\widetilde{C}_A^K = C_A^K = \frac{3\pi^2}{16}\frac{1}{T_K^2} \quad (B = 0), \tag{34a}$$

and asymptotic large-field behavior [obtained via (18)]

$$\begin{Bmatrix} \widetilde{C}_A \\ C_A \end{Bmatrix} = \pm\frac{\pi^2}{B^2(\ln\beta_r)^4}\ln\beta_r \quad (B \gg T_K). \tag{34b}$$

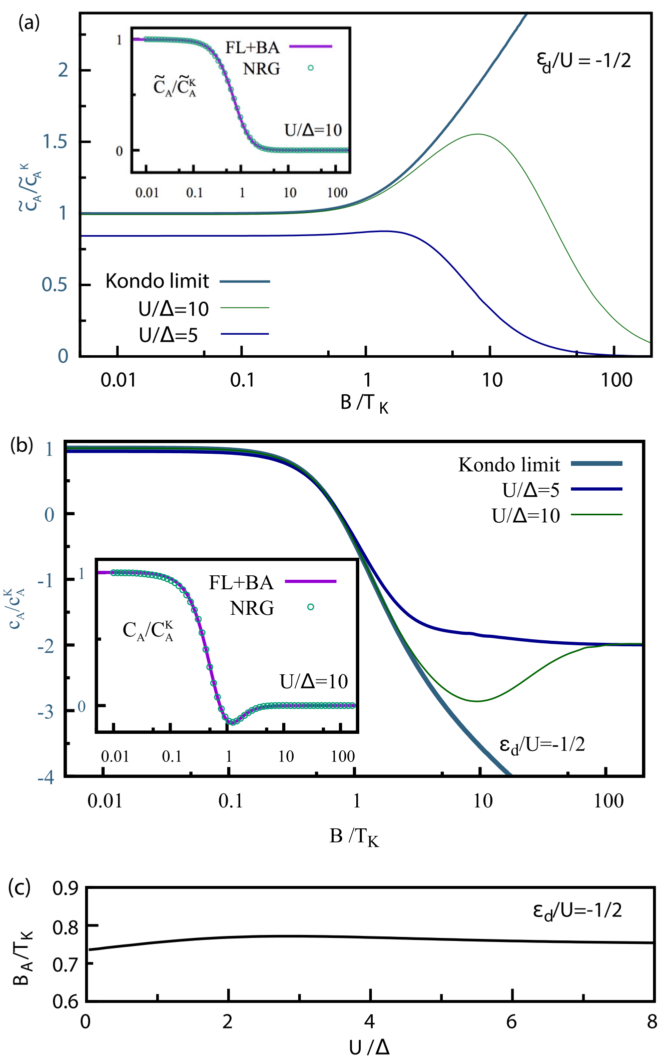

FIG. 1. Low-energy properties of the spectral function at particle-hole symmetry. (a) The normalized height coefficient $\tilde{c}_A/\tilde{c}_A^K$ and (b) curvature coefficient c_A/c_A^K of the local spectral function at particle-hole symmetry, plotted as functions of magnetic field [in units of T_K, as defined in Eq. (20)], for three values of the interaction parameter U/Δ, including the Kondo limit $U/\Delta = \infty$ [given by Eq. (35)]. The insets of (a) and (b), respectively, show $\widetilde{C}_A/\widetilde{C}_A^K$ and C_A/C_A^K as functions of B/T_K, calculated from our FL predictions [Eq. (32)] (solid lines), and by computing the spectral function via NRG and extracting its zero-energy height and curvature (open circles). The sign change for C_A signals the splitting of the Kondo resonance into two resonances due the breaking of the Kondo singlet by the magnetic field. (c) The characteristic field B_A where C_A vanishes, plotted in units of T_K as function of U/Δ. In the Kondo limit $U/\Delta \to \infty$ it approaches the value $B_A/T_K = 0.75073$.

This confirms that C_A is negative at large fields while $\widetilde{C}_A$ remains positive. They have equal magnitudes in both the limits $B = 0$ and $B \gg T_K$, changing in scale from $\sim 1/T_K^2$ to becoming negligibly small, $\sim 1/[B^2(\ln\beta_r)^3]$. We now also see why it is useful to study the C coefficients in the normalized form $c = E_*^2 C$ of Eq. (31), as done in Fig. 1: E_*^2 increases with B and in the large-field limit [see (21)] compensates the small prefactor in Eq. (34b). Correspondingly normalized, Eqs. (33) and (34) yield

$$\begin{Bmatrix} \tilde{c}_A/\tilde{c}_A^K \\ c_A/c_A^K \end{Bmatrix} = \cos(2\pi m_d) \mp \frac{\partial_B \chi_s}{3\pi\chi_s^2}\sin(2\pi m_d)\,, \tag{35}$$

with zero-field values and large-field behavior given by

$$\tilde{c}_A^K = c_A^K = \frac{3\pi^2}{16}, \quad (B=0), \tag{36a}$$

$$\begin{Bmatrix} \tilde{c}_A/\tilde{c}_A^K \\ c_A/c_A^K \end{Bmatrix} = \pm\frac{1}{3}\ln\beta_r(B \gg T_K)\,. \tag{36b}$$

The $\pm\ln\beta_r$ term in Eq. (36b) explains the behavior of the Kondo limit curves (thick solid) in Figs. 1(a) and 1(b).

As a consistency check, we note that inserting the Kondo-limit coefficients $\widetilde{C}_A^K$ and C_A^K of Eq. (34a) into Eq. (26) for $A(\varepsilon)$ yields the low-energy expansion of the spectral function of the spin-$\frac{1}{2}$ Kondo model at $B = 0$. Indeed, the result so obtained,

$$A^K(\varepsilon) = 2 - \frac{3\pi^2}{16}\frac{\left[\varepsilon^2 + \frac{1}{3}(\pi T)^2 + \frac{1}{4}(eV)^2\right]}{T_K^2}\,, \tag{37}$$

is consistent with previous studies of the Kondo model for $V = 0$ [32,39,49,64] [see for example Eq. (4) of Ref. [39], where the coefficients of this expansion, called c_ε and c_T' there, were checked numerically using NRG].

For completeness, we mention that the opposite limit of weak interactions yields, for $\varepsilon_d = U = 0$:

$$\tilde{c}_A = 0, \quad c_A = \frac{\pi^2}{8}\frac{\Delta^2 - 3B^2/4}{\Delta^2 + B^2/4}\,. \tag{38}$$

C. Conductance at particle-hole symmetry

We now turn our attention to transport properties, and again begin with a qualitative discussion. The behavior of the local spectral function discussed in the preceding subsection fully determines, via the Meir-Wingreen formula (23), that of the nonlinear differential conductance. At zero field $G(V,T)$, studied as function of V, exhibits a peak around zero bias, which weakens with temperature, and which splits with increasing field. The details of these changes are governed by a sensitive interplay of two effects: increasing temperature or bias from zero (i) on the one hand weakens the Kondo peaks, thus causing a height reduction of $A(0)$, but (ii) on the other hand widens the energy window over which the spectral function is probed, set by the $f_L - f_R$ factor in the Meir-Wingreen formula ("window widening"). Whereas height reduction tends to reduce the conductance, window widening can either reduce or enhance it, depending on whether $A(\varepsilon)$ has a maximum or minimum around zero, as is the case for small or large fields, respectively. For small fields, height reduction and window widening act together to reduce the conductance when T or V are increased from zero. For large fields, however, they counteract each other, and *if* window widening dominates, the conductance will increase with T or V.

The interplay of height reduction (governed by $\tilde{c}_A$) and window widening (governed by c_A) is quantified by Eq. (30): as $\tilde{c}_A$ and c_A decrease with increasing field, with $\tilde{c}_A$ remaining

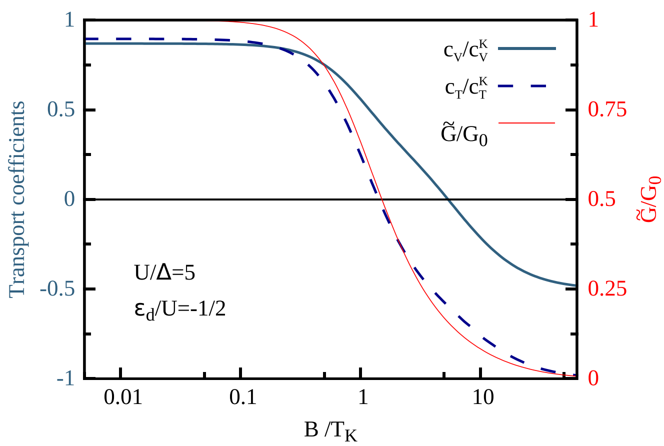

FIG. 2. FL transport properties at particle-hole symmetry and $U/\Delta = 5$, plotted as functions of B/T_K. Left axis: Normalized FL transport coefficients c_V/c_V^K (thick solid line) and c_T/c_T^K (thick dashed line). The field B_T where c_T changes sign is of order T_K (slightly larger but comparable to B_A), whereas the field B_V where c_V changes sign is much larger, of order $\sqrt{U\Delta}$. Right axis: Normalized zero-temperature linear conductance $\tilde{G}/G_0 = \cos^2(\pi m_d)$ [from Eq. (32a)] (thin solid line).

positive and c_A turning negative, c_T and c_V will decrease too, but turn negative only if the contribution from c_A (window widening) outweighs that from $\tilde{c}_A$ (height reduction). We will denote the "splitting fields" at which c_T or c_V equal zero by B_T or B_V, respectively. Since in Eq. (30) the relative weight of $\tilde{c}_A$ to c_A is three times larger in c_V than in c_T, the influence of height reduction compared to window widening is larger for c_V than for c_T. The general behavior of these two coefficients, and that of the corresponding splitting fields B_V and B_T, can thus differ significantly.

In the noninteracting limit, where $\tilde{c}_A = 0$, c_T, c_V and c_A are proportional to each other for all fields, $c_V = \frac{3}{4\pi^2}c_T = \frac{1}{4}c_A$, implying splitting fields of $B_T = B_V = (2/\sqrt{3})\Delta$ [see Eq. (38)]. At this field value, the magnetization equals $\frac{1}{6}$ and the zero-temperature linear conductance is $\widetilde{G} = \frac{3}{2}e^2/h$, i.e., $\frac{3}{4}$ of the unitary value $G_0 = 2e^2/h$.

With increasing U/Δ, the behavior of c_T and c_V becomes increasingly dissimilar. This is already evident in Fig. 2, which shows the B dependence of $\widetilde{G}$, c_T and c_V for $U/\Delta = 5$. With increasing field, $\widetilde{G}$ is smoothly suppressed on a field scale set by T_K, while c_T and c_V both decrease and change sign, albeit at rather different field scales: B_T is of order T_K (slightly larger but comparable to B_A), whereas B_V is of order $\sqrt{U\Delta}$, which is much larger than T_K. The large-field values reached by c_T and c_V for $B \gg \sqrt{U\Delta}$ are also different. For U/Δ not too large ($\lesssim$5, as in Fig. 2), they correspond to the empty-orbital asymptotic forms found in Ref. [47],

$$c_T^{\mathrm{eo}} = -\frac{\pi^4}{16}, \qquad c_V^{\mathrm{eo}} = -\frac{3\pi^2}{64}. \tag{39}$$

A systematic study of the splitting fields B_T and B_V as functions of U/Δ yields the results shown in Fig. 3. They differ strikingly. On the one hand, the splitting field B_T shown in Fig. 3(a) remains of order T_K for all values of U/Δ. This implies that B_T is *universal* in the same sense as B_A, although

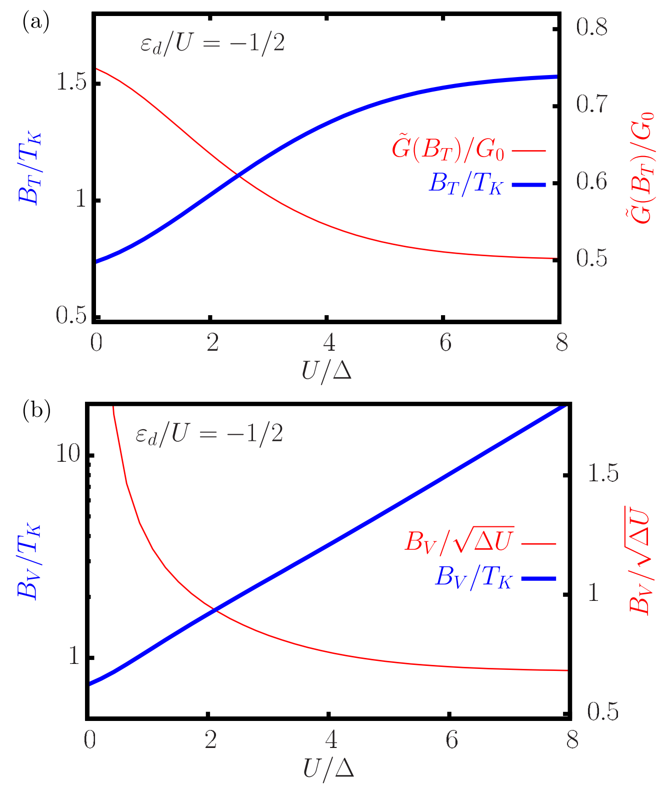

FIG. 3. Interaction dependence of splitting field properties at particle-hole symmetry, plotted as functions of U/Δ. (a) Splitting field B_T at which c_T vanishes (left axis, thick line), shown in units of T_K, and the normalized zero-temperature linear conductance at that field, $\widetilde{G}(B_T)/G_0$ (right axis, thin line). (b) The splitting field B_V at which c_V vanishes, shown in units of both T_K (left axis, thick line, log scale) and $\sqrt{U\Delta}$ (right axis, thin line, linear scale). For strong interactions $U \gg \Delta$, we find $B_V = 0.679\sqrt{U\Delta}$, implying that $B_V \gg B_T$. In the absence of interaction $U = 0$, the Kondo temperature extracted from Eq. (20) is $T_K = \pi\Delta/2$, hence $B_V/T_K = \frac{4}{\pi\sqrt{3}} \simeq 0.735$.

the dependence on U/Δ is somewhat stronger for B_T/T_K than for B_A/T_K in Fig. 1(c). In contrast, the splitting field B_V shown in Fig. 3(b) exhibits *nonuniversal* behavior, crossing over from order T_K to order $\sqrt{U\Delta}$ as U/Δ increases from $\lesssim 1$ to $\gg$1. For fields as large as $\sqrt{U\Delta}$, i.e., well above the value $B_A \simeq T_K$ where the peak splitting of the spectral function becomes discernible, charge fluctuations are not small, suggesting that for large interactions the sign change in c_V is driven not by Kondo physics but by the onset of charge fluctuations. Consequently, we expect that in the Kondo limit $U/\Delta \to \infty$, where charge fluctuations are strictly suppressed, c_V will never change sign, implying $B_V = \infty$. This is indeed the case, as seen in Fig. 4, which shows the evolution of c_V as function of field for a series of increasing U/Δ values, including the Kondo limit.

In the Kondo limit, Eqs. (30), (33), and (34) yield

$$c_T/c_T^K = \cos(2\pi m_d), \tag{40a}$$

$$c_V/c_V^K = \cos(2\pi m_d) - \frac{\partial_B \chi_s}{6\pi\chi_s^2}\sin(2\pi m_d), \tag{40b}$$

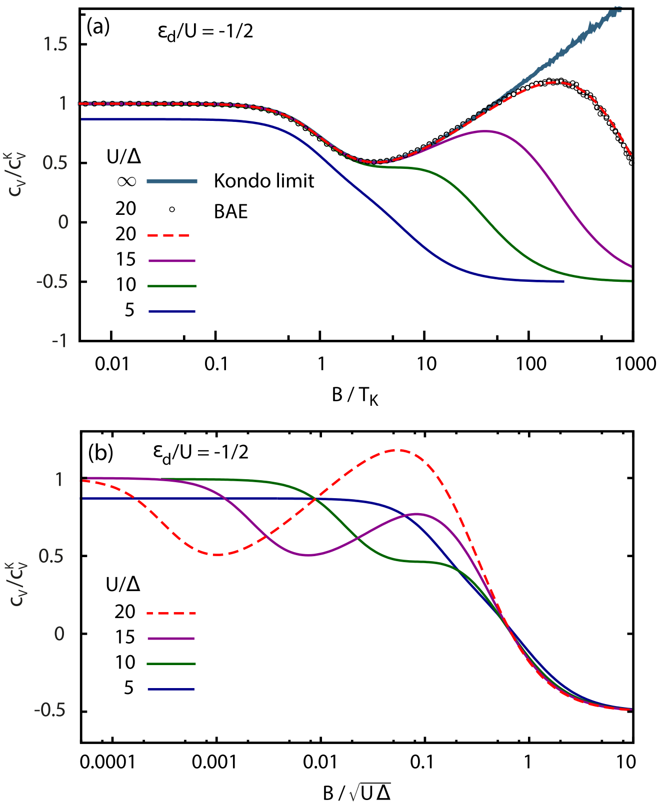

FIG. 4. Evolution of c_V during the crossover to the Kondo limit. (a) The normalized FL transport coefficient c_V/c_V^K, plotted as a function of B/T_K for several values of U/Δ, including the Kondo limit (thick solid line). For the latter, c_V is strictly positive for all magnetic fields. The direct integration of the coupled Bethe ansatz equations, Eq. (S3a) and (S4b) [65], performed here for $U/\Delta = 20$ (BAE, open dots), is in very good agreement with the corresponding Wiener-Hopf solution (dashed line). All curves with large U/Δ ($\gtrsim$10) initially collapse onto a universal scaling curve as function of increasing B/T_K, but for large B eventually bend downward and change sign. (b) Same as (a), but plotted as function of $B/\sqrt{U\Delta}$. Now a scaling collapse sets in at magnetic fields larger than $\sqrt{U\Delta}$, which is thus seen to be the field scale beyond which c_V changes sign. Together, these two panels show that as long as B is smaller than the high-energy scale $\sqrt{U\Delta}$ of the Anderson model, c_V shows universal behavior, governed by a single scale T_K and characteristic of the Kondo model, and in this Kondo regime, c_V remains strictly positive.

with zero-field values and large-field behavior given by

$$c_T^K = \frac{\pi^4}{16}, \quad c_V^K = \frac{3\pi^2}{32}, \quad (B = 0), \tag{41a}$$

$$c_T = -c_T^K, \quad c_V = c_V^K \frac{1}{6} \ln \beta_r, \quad (B \gg T_K). \tag{41b}$$

Thus c_T changes sign when the magnetization crosses $m_d = \frac{1}{4}$, in which case the zero-temperature linear conductance is $\tilde{G} = \frac{1}{2}G_0$, half the unitary value. The corresponding magnetic field, obtained from Bethe ansatz in the Kondo limit, is $B_T/T_K = 1.54813$. In contrast, c_V does not change sign and remains positive in the large-field limit, indeed implying $B_V = \infty$. This, and the fact that $B_A < B_T$, can be understood by comparing Eqs. (35) and (40): the $(\partial_B \chi_s/\chi_s^2)$ term that yields $\ln \beta_r$ at large fields is strictly negative for c_A, absent for c_T and strictly positive for c_V. Note that Eq. (41b) implies that the unnormalized coefficients C_T and C_V both vanish in the large-field limit, as $1/[B^2(\ln \beta_r)^4]$ and $1/[B^2(\ln \beta_r)^3]$, respectively.

According to the above analysis the value of the zero-temperature linear conductance at the temperature splitting field, $\widetilde{G}(B_T)$, decreases from $\frac{3}{4}G_0$ to $\frac{1}{2}G_0$ when U/Δ increases from zero to infinity. This is illustrated by the red thin line in Fig. 3(a).

Let us summarize the two most striking features found above: (i) The splitting field B_V is not universal, crossing over from order T_K to order $\sqrt{U\Delta}$ as U/Δ increases past 1. Thus contrary to initial expectations, the field B_V where the zero-bias maximum turns into a minimum is parametrically different from the field $B_A \simeq T_K$ where the Kondo resonance in the spectral function splits. (ii) In the Kondo limit C_V, though decreasing towards zero with increasing field, never becomes negative, hence the conductance maximum at zero bias, though shrinking and flattening to the point of becoming undiscernable, *never* changes into an actual minimum, no matter how large the field. The cause of these features is that increasing U/Δ strongly tilts the interplay between bias-induced height reduction of $A(0)$ and window widening in favor of the former.

How can these findings be reconciled with the well-established fact that for the Kondo model (i.e., the $U/\Delta \to \infty$ limit of the Anderson model) the nonlinear conductance at large magnetic field shows two well-defined "large-bias" peaks at $eV \simeq \pm B$ [modulo corrections of order $\ln(B/T_K)$]? First note that the occurrence of large-bias conductance peaks, found by perturbative calculations in $1/\ln(V/T_K)$ for $V/T_K \gg 1$ [12,31], does not contradict our analysis, which is limited to the opposite regime of small bias. Nevertheless, as large-bias peaks are absent at zero or small field, it is interesting to speculate how they emerge when the field is turned on. They cannot emerge near $V \simeq 0$ from a field-induced splitting of the zero-bias peak into two subpeaks that drift apart with increasing field, because that would contradict our finding (ii) that no zero-bias minimum ever appears. Instead, we expect that once the field increases well past T_K, two conductance shoulders will emerge near *finite* $eV \simeq \pm B$ in the flanks of the zero-bias peak, which subsequently develop into two well-defined local maxima as the magnetic field is further increased, while the zero-bias peak shrinks and flattens but remains a local maximum throughout. However, the latter will become very weak, since $C_V \to 0$ when $B \to \infty$, as shown in Fig. 5. We thus expect a plot of $G(V)$ versus V at large B to show two finite-bias maxima separated by a valley, whose curvature, positive in the flanks of the two maxima, turns negative near $V = 0$, but is so small in magnitude there that for practical purposes the valley will appear to be flat at its center.

For the Anderson model with $U \gg \Delta$, where B_V is not infinite but large, we expect a similar scenario: with increasing field the zero-bias conductance maximum initially weakens without splitting; once B passes T_K, two additional finite-bias peaks emerge from the flanks of the central peak, near $eV \simeq \pm B$, while the zero-bias maximum keeps shrinking and flattening; and much later, when B finally

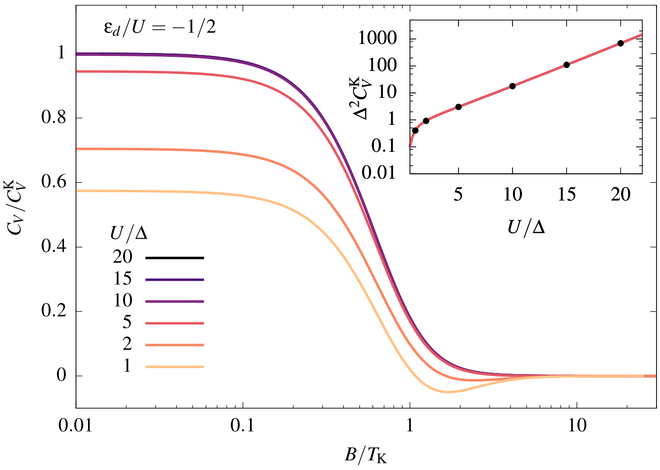

FIG. 5. The coefficient $C_V = c_V/E_*^2$, plotted as a function of B/T_{K} for different interaction strengths U/Δ, in units of $C_V^{\mathrm{K}} = c_V^{\mathrm{K}}/T_K^2$, with c_V^{K} defined in Eq. (41a). In contrast to c_V from Fig. 4(a), C_V is strongly suppressed in the regime $B > T_K$ (even for $U/\Delta \gg 1$), because for large fields the spin susceptibility becomes very small and hence E_* very large [cf. Eq. (21)]. Inset: the normalization factor C_V^{K}, plotted as function of U/Δ in units of $1/\Delta^2$ (black points indicate the U/Δ values from the main plot). C_V^{K} shows an exponential increase with U/T_K, caused by an exponential decrease in T_K. The growth in C_V^{K} is counteracted by the fact that the voltage window in which our FL analysis applies decreases exponentially, since the FL expansion (29) of the conductance requires $V \ll T_K$.

passes $B_V \sim \sqrt{U\Delta}$, the zero-bias maximum turns into a minimum and only the two large-bias peaks remain. Thus the appearance of two finite-bias side peaks does not go hand in hand with the appearance of a zero-bias minimum, but well precedes it.

To conclude this section, we remark that our conclusion that $B_V = \infty$ in the Kondo limit disagrees with Ref. [30], where renormalized perturbation theory (RPT) for the case of particle-hole symmetry yielded a finite value for B_V in the Kondo limit [see the discussion after their Eqs. (19) and (27)]. Their results differ from ours also for finite values of U/Δ; for example, for $U/\Delta = 4\pi$ they find $\frac{1}{2}B_V \simeq 0.584 T_K$ [after their Eq. (27)], whereas we find $B_V \simeq 0.679\sqrt{U\Delta}$ [see our Fig. 3(b)]. In Ref. [30], the coefficients playing the roles of our $\alpha_{2\sigma}$ and $\phi_{2\sigma}$ are computed perturbatively in terms of the renormalized parameters of RPT (the *same* three parameters are also used at zero magnetic field [41]), and are therefore approximate. As noted in the concluding section of Ref. [47], it is not clear whether this RPT approach contains enough parameters to accurately evaluate B_V.

To try to identify the origin of the disagreement, we have expressed our FL parameters in terms of the RPT parameters needed in general to characterize the local impurity Green's function (see Appendix B). This can be done by simply expanding the RPT spectral function to second order in ε, T, and eV and equating the result to our Eqs. (26) and (27). The resulting equations (B8) provide a RPT-FL dictionary that relates the RPT parameters to our FL parameters. Since the latter are computable exactly via the Bethe ansatz, this dictionary provides a number of exact constraints on the RPT parameters. We were not able to ascertain that the expressions provided in Ref. [30] for their RPT parameters satisfy these constraints. We suspect that at finite magnetic field or out of particle-hole symmetry, the second-order RPT (perturbative in the renormalized interaction U) becomes approximate for the calculation of the coefficients α_2 and ϕ_2 [82]. However, we would like to suggest a converse strategy: one could set up a RPT whose input parameters are computed exactly by Bethe ansatz via the RPT-FL dictionary in Appendix B. Doing so would be an interesting goal for future work, since RPT offers the welcome prospect of smoothly linking the exact FL description of the impurity's low-energy behavior to a description, albeit approximate, that is also useful at higher energies.

D. c_V away from particle-hole symmetry

Finally, let us examine the behavior of the transport coefficient c_V away from particle-hole symmetry. We consider only $\varepsilon_d/U > -\frac{1}{2}$ (from which the opposite case follows by particle-hole symmetry). The quantum dot is in a strongly correlated Kondo singlet state as long as the dot is in the local-moment regime ($-U/2 \leqslant \varepsilon_d \lesssim -\Delta$). As ε_d crosses over through the mixed-valence regime ($|\varepsilon_d| < \Delta$) into the empty-orbital regime ($\varepsilon_d \gtrsim \Delta$), Kondo correlations die out completely. In the previous section, we showed that c_V changes sign at particle-hole symmetry for splitting fields B_V of the order of $\sqrt{U\Delta}$ [see Fig. 3(b)]. Our aim here is to study the evolution of B_V as ε_d/U is tuned through the transition from the local-moment regime to the empty-orbital regime. The numerical results reported below were obtained by numerically solving the Bethe ansatz equations for the Anderson model [64,83] in the form reported in Ref. [65].

Figure 6(a) shows a color-scale plot of c_V for a large, fixed interaction of $U/\Delta = 20$, plotted as function of field B and level energy ε_d. Figure 6(b) shows the same data as function of B along several fixed values of ε_d. We find that throughout the local-moment regime, an increasing field yields an initial minimum for c_V as function of B around field values that distinctly follow the ε_d dependence of the Kondo temperature T_K of Eq. (20) (grey triangles). The latter is well approximated by the analytic formula $T_K^{(\mathrm{af})}$ of Eq. (22) (black solid line) and coincides with the FL scale E_* of Eq. (19) at $B = 0$ (grey squares), with deviations only in the empty orbital regime ($\varepsilon_d \gtrsim \Delta$). Just as in the previous section, we observe an actual change of sign for c_V (indicated by black dots) only at fields B_V much higher than T_K. Close to particle-hole symmetry B_V scales as $\sqrt{U\Delta}$ [cf. Fig. 3(b)], crossing over to values of order Δ when approaching the empty orbital regime.

The behavior of c_V is strongly modified as soon as the renormalized level increases past the Fermi surface ($\varepsilon_d \gtrsim \Delta$) and the charge on the dot changes from 1 to 0, so that Kondo correlations are completely absent. For low magnetic fields, c_V is negative and with increasing field evolves through a double sign change with a positive-valued peak in between, see Figs. 6 and 7. This behavior can be understood as follows. At zero magnetic magnetic field, the dot is empty and in a cotunneling regime [84], so that its conductance increases when the bias increases from zero. This explains why c_V is found to be negative for small fields in Fig. 6. With increasing field, the local level is Zeeman split. When

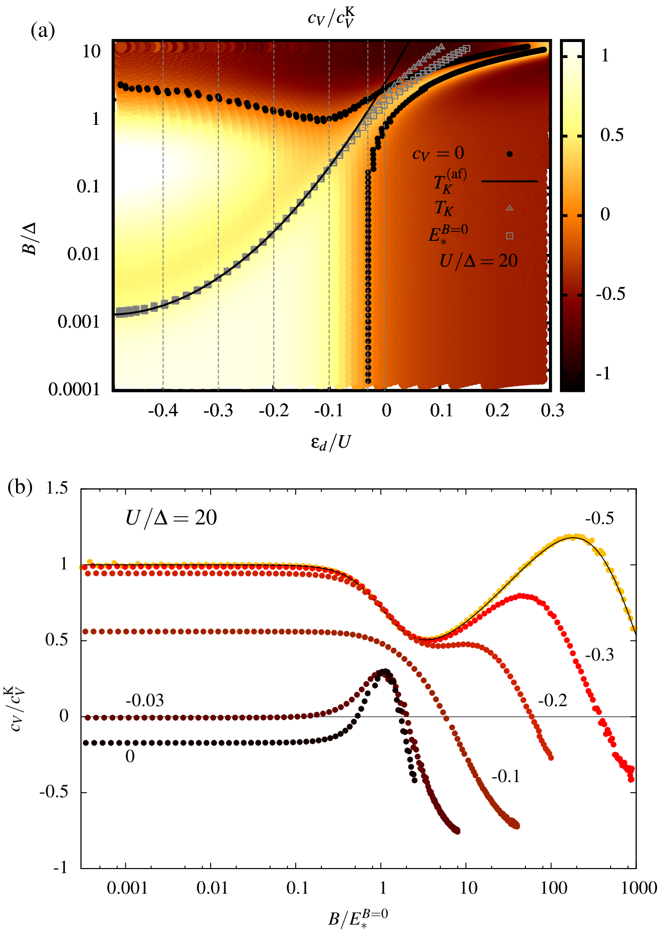

FIG. 6. (a) Transition from the local-moment regime to the empty-orbital regime for the transport coefficient c_V/c_V^K, shown using a color scale, as a function of the magnetic field B and the level energy ε_d, at $U/\Delta = 20$, a convenient value to highlight features related to Kondo physics. The solid line shows the prediction for the Kondo scale of the analytic formula (22) for $T_K^{(\rm af)}$, the grey triangles the numerical evaluation of T_K as defined in Eq. (20) and the grey squares the numerical evaluation of E_* in Eq. (19) for $B = 0$. All these quantities show a nice agreement as long as $\varepsilon_d < 0$. The black points signal when $c_V = 0$ and changes sign. The light-colored regions correspond to positive values of c_V. (b) Same quantity c_V/c_V^K as in (a), now shown along the cuts marked in (a) by grey dashed lines, and plotted as a function of $B/E_*^{B=0}$ on a logarithmic scale. The numbers above the data points give the corresponding values of ε_d/U (increasing as colors turn from light to dark). The solid line corresponds to the analytical result for c_V at particle-hole symmetry derived from the Wiener-Hopf solution [65] [see also Fig. 4(a)]. Throughout the local-moment regime in which Kondo correlations occur ($\varepsilon_d \lesssim -\Delta$), c_V shows a local minimum around fields of order T_K, and changes sign only at a much larger field, $B_V \gg T_K$. For $\varepsilon_d \gtrsim 0$, c_V develops a double sign change with a peak in between, which reflects a field-induced resonance between the empty- and singly occupied dot states (see Fig. 7).

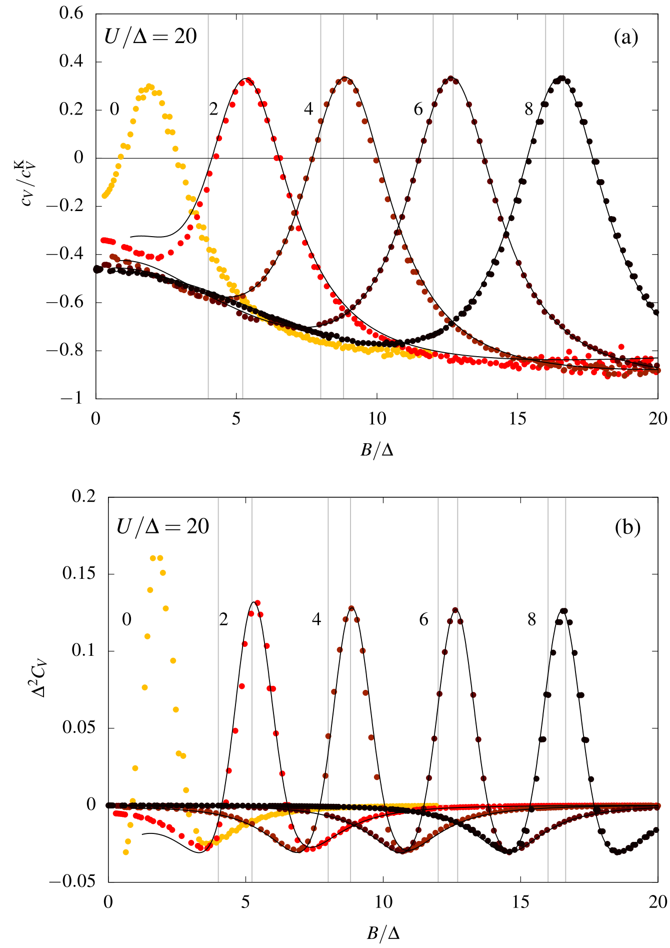

FIG. 7. Magnetic-field dependence of (a) c_V in units of $c_V^{\rm K}$ and (b) $C_V = c_V/E_*^2$ in units of $1/\Delta$, in the mixed-valence and empty-orbital regimes. Both are plotted as functions of B/Δ on a linear scale, for several values of ε_d/Δ (given by numbers above the data points, increasing as colors turn from light to dark). Black solid curves display analytical predictions derived in perturbation theory, showing good agreement with the numerical results (symbols). The peaks in c_V and C_V reflect the field-induced resonance between the empty and singly occupied dot states. Vertical solid lines indicate the predicted values of the resonance field, $B = 2\tilde{\varepsilon}_d$, where the renormalized level position $\tilde{\varepsilon}_d$ is given by Eq. (42) (and $\alpha \simeq 1.62$ therein); for comparison, vertical dashed lines indicate the bare values, $B = 2\varepsilon_d$. Note that the nontrivial B dependence exhibited by C_V in (b) is as pronounced as that of c_V in (a). The reason is that near the resonance field $B \simeq 2\tilde{\varepsilon}_d$, both the spin and charge susceptibilities are large, ensuring that E_* remains small.

the empty and singly occupied states come into resonance, the conductance develops a well-pronounced zero-bias peak with a negative curvature, explaining why c_V goes through a positive-valued maximum. The resonance condition at which this happens is that the spin-up Zeeman energy $B/2$ matches the renormalized level position $\tilde{\varepsilon}_d$, which differs from ε_d due to virtual processes involving doubly occupied intermediate dot states. A perturbative calculation following Haldane [66] yields [85]

$$\tilde{\varepsilon}_d = \varepsilon_d + \frac{\Delta}{\pi} \ln \frac{\varepsilon_d + U}{\alpha \varepsilon_d}, \tag{42}$$

where α is a constant of order one. For the choice $\alpha \simeq 1.62$, the resonance field values $B = 2\tilde{\varepsilon}_d$, indicated by vertical solid lines in Fig. 7, indeed match the observed peak positions for c_V rather well.

For $\varepsilon_d > \Delta$, the full dependence of c_V on the magnetic field can be well captured analytically by second-order perturbation theory in the dot-lead hybridization [86], using the spin-down state of the dot as virtual intermediate state. Appendix C presents corresponding results for $n_{d\sigma}$ as function of the bare level position ε_d and Zeeman field B, from which c_V can be obtained using the formulas of Sec. II. Using the substitution $\varepsilon_d \to \tilde{\varepsilon}_d$ in the final results, one obtains the solid curves for c_V shown in Fig. 7, which agree nicely with our numerical results (symbols). In the limit $\varepsilon_d \gg \Delta$, where the spin-down state can be totally neglected, the shape of the c_V peak can be computed by considering a single noninteracting resonant level. The result is

$$\frac{c_V}{c_V^{\mathrm{K}}} = \frac{1}{3}\frac{\Delta^2 - 3\left(\frac{1}{2}B - \varepsilon_d\right)^2}{\Delta^2 + \left(\frac{1}{2}B - \varepsilon_d\right)^2}, \tag{43}$$

which is peaked symmetrically around the resonance field $B = 2\varepsilon_d$.

In the mixed-valence and empty-orbital regimes, the nontrivial B-dependence exhibited by c_V is equally well visible in $C_V = c_V/E^{*2}$, see Fig. 7(b) (in contrast to the Kondo regime, where C_V rapidly approaches zero for $B \gtrsim T_K$, cf. Fig. 5). The reason is that in the mixed-valence and empty-orbital regimes the FL scale E_* does *not* become very large with increasing B, because both the spin and charge susceptibilities χ_s and χ_c are sizable, ensuring that E_* remains small [cf. Eq. (19)]. In fact, both susceptibilities become maximal, and E_* minimal, in the regime near near $B \simeq 2\tilde{\varepsilon}_d$ where the empty and singly occupied dot states are in resonance. This can be checked analytically in the $\varepsilon_d \gg \Delta$ limit, where the perturbative approach presented in Appendix C yields

$$E_* = \frac{\pi}{2\Delta}[(\varepsilon_d - B/2)^2 + \Delta^2], \tag{44}$$

which is *minimal* at the bare resonance field $B = 2\varepsilon_d$. The fact that C_V is large in the mixed-valence and empty-orbital regimes suggests that these regimes would be particularly suitable for the purposes of benchmarking numerical methods for solving the nonequilibrium Anderson model against the exact results obtained by our FL approach.

IV. SUMMARY AND CONCLUSIONS

We extended the FL framework of Ref. [47] to the single-impurity Anderson model at finite magnetic field where low-energy properties can be calculated in the whole phase diagram. Using a generalization of the “floating Kondo resonance” argument of Nozières, we expressed all parameters of the low-energy effective FL Hamiltonian in terms of the zero-temperature local occupation functions $n_{d\sigma}$ and their derivatives with respect to level energy and magnetic field, and evaluated these using precise Bethe ansatz calculations. Focussing on strong interaction, zero temperature and particle-hole symmetry where the Kondo singlet forms, we obtained exact results for the magnetic-field dependence of $\tilde{c}_A$ and c_A, two parameters that characterize the zero-energy height and curvature of the equilibrium spectral function, respectively. Direct NRG computations of the spectral function quantitatively confirm our FL results for $\tilde{c}_A$ and c_A, thereby establishing the soundness of our FL theory. We also computed the splitting field B_A at which c_A changes sign, signaling the onset of a field-induced splitting of the equilibrium Kondo peak, and find that B_A is of order T_K throughout the local-moment regime, as expected.

We next performed exact calculations of the FL transport coefficients c_T and c_V at particle-hole symmetry but for arbitrary magnetic fields. In the local-moment regime, we find that c_T changes sign at a field B_T of order T_K, as expected, but c_V changes sign only at a parametrically larger field B_V of order $\sqrt{U\Delta}$. This unexpected result implies that the emergence of finite-bias side peaks in the nonlinear conductance at field scales of order T_K (reflecting the peak splitting of the spectral function) is not accompanied by a simultaneous change of the zero-bias maximum into a minimum—the latter change occurs only at much larger fields, of order $\sqrt{U\Delta}$, indicative of the onset of charge fluctuations. In the Kondo model, which does not account for charge fluctuations at all, the zero-bias maximum, though becoming increasingly flat with increasing field, never turns into a minimum, no matter how large the field. The fact that the splitting field B_V for the conductance is so much larger than the splitting field B_A for the spectral function implies that the zero-bias curvature of the nonlinear conductance is not a good diagnostic tool for the field-induced splitting of the spectral function, contrary to initial expectations. The reason is that this zero-bias curvature results from an interplay of two effects, namely a bias-induced reduction in the zero-energy height $A(0)$ of the spectral function, which tends to reduce the conductance, and a bias-induced widening of the transport window, which tends to increase the conductance if the spectral function is split. The former effect turns out to outweigh the latter for all fields up to the scale $\sqrt{U\Delta}$, where charge fluctuations begin to contribute.

Finally, we also calculated the magnetic-field dependence of c_V throughout the crossover from the local-moment through the mixed-valence into the empty-orbital regime. Throughout the former, the behavior of c_V is qualitatively similar to that found at particle-hole symmetry. However, it changes dramatically upon entering the empty orbital regime: there c_V is negative at zero magnetic field, but with increasing field traverses a positive-valued peak at twice the renormalized level energy, $B \simeq 2\tilde{\varepsilon}_d$, arising from a spin-polarized resonance between the empty and singly occupied dot states.

It would be an interesting challenge for experimental studies of nonequilibrium transport through quantum dots to check our peak-splitting predictions by detailed measurements of the nonlinear conductance as function of bias voltage and field. Since the specifics of our peak-splitting predictions are model dependent, it would be important to strive for a faithful implementation of the *single-level* Anderson model, requiring a small dot with a very large level spacing, and to make the ratio U/Δ as large as possible.

To conclude, we have used exact tools to address the question posed in the title of our paper, coming to the surprising conclusion that it has two qualitatively very different answers, depending on whether one studies the spectral function or the nonlinear conductance. On a quantitative level, our work establishes exact benchmark results against which any future numerical work on the nonequilibrium properties of the Anderson model can be tested.

ACKNOWLEDGMENTS

We thank S. Arlt, M. Kiselev, H. Schoeller, D. Schimmel, A. Weichselbaum, and L. Weidinger for helpful discussions, and A. Hewson for several very helpful exchanges on renormalized perturbation theory. This work has been supported by the DFG through the Cluster of Excellence "NanoSystems Initiative Munich."

APPENDIX A: KONDO MODEL AT LARGE MAGNETIC FIELD

In this appendix, we perform a consistency check of the FL theory of the main text by considering the Kondo model in the large-field limit $B \gg T_K$. To this end, we derive an effective FL Hamiltonian from the Kondo Hamiltonian by doing second-order perturbation theory in spin-flip scattering. This yields explicit expressions, in terms of the *bare* parameters of the Kondo model, for the FL parameters $\delta_{0\sigma}$, $\alpha_{j\sigma}$ and $\phi_{j\sigma}$, and hence, via the FL relations (13), also for m_d, χ_s and $\partial\chi_s/\partial B$. Satisfyingly, the latter expressions turn out to fully agree with corresponding Bethe ansatz results in the large-field limit.

A standard mapping exists between the Anderson model Eq. (1) and the Kondo model $H_K = -B\,S_z + \sum_{\sigma,k}\varepsilon_k c^\dagger_{k\sigma}c_{k\sigma} + H_{\rm ex}$ with the spin-exchange interaction

$$H_{\rm ex} = J\,\mathbf{S}\cdot\mathbf{s}, \tag{A1}$$

where $\mathbf{s} = \sum_{kk'\sigma\sigma'} c^\dagger_{k\sigma}\frac{\boldsymbol{\tau}_{\sigma\sigma'}}{2}c_{k'\sigma'}$ denotes the local spin of conduction electrons and $\boldsymbol{\tau}_{\sigma\sigma'}$ is a vector composed of the Pauli matrices. The mapping holds at particle-hole symmetry, where $\nu_0 J = 8\Delta/(\pi U)$, and for energies well below the charging energy U. The impurity then hosts exactly one electron with spin $\mathbf{S}$.

The FL Hamiltonian of Eq. (3) can be derived perturbatively at large magnetic fields $B \gg T_K$. A strong magnetic field polarizes the impurity and a perturbation expansion with respect to the impurity in the spin up state $|\uparrow\rangle$ can be formulated. The result is a perturbative Hamiltonian $H_{\rm pert} = H_1 + H_2 + \ldots$ written as a series with increasing powers of J, and in which the impurity spin has disappeared. The leading order H_1 is simply obtained by averaging the exchange Kondo term over the spin-up state,

$$H_1 = \langle\uparrow|H_{\rm ex}|\uparrow\rangle = \frac{J}{4}\sum_{\sigma,k,k'}\sigma c^\dagger_{k\sigma}c_{k'\sigma}, \tag{A2}$$

corresponding to a spin-selective potential scattering term inducing the phase shifts $\delta_{0\uparrow} = \pi - \pi\nu_0 J/4$ and $\delta_{0\downarrow} = \pi\nu_0 J/4$. The next order, H_2, arises from virtual impurity spin-flip process in which an electron-hole pair (with opposite spins) is excited. It is obtained by using the standard Schrieffer-Wolff technique, with the outcome

$$H_2 = -\frac{J^2}{8}\sum_{\{k_i\}}\frac{1}{B+\varepsilon_3-\varepsilon_4}c^\dagger_{k_1\downarrow}c_{k_2\uparrow}c^\dagger_{k_3\uparrow}c_{k_4\downarrow} + \text{H.c.} \tag{A3}$$

In order to compare this result with the FL form of Eq. (3), we normal order the two equal-spin pairs of operators in Eq. (A3) with respect to a reference ground state with spin-dependent chemical potentials $\varepsilon_{0\sigma} = -\frac{1}{2}\sigma B_0$ close to $\mu_{0\sigma} = 0$ (in the Kondo limit, where $\varepsilon_d = -\infty$, there is no need to use $\varepsilon_0 \neq 0$):

$$c_{k_2\uparrow}c^\dagger_{k_3\uparrow} = -:c^\dagger_{k_3\uparrow}c_{k_2\uparrow}: + \delta_{k_3,k_2}\theta(\varepsilon_2-\varepsilon_{0\uparrow}), \tag{A4a}$$

$$c^\dagger_{k_1\downarrow}c_{k_4\downarrow} = :c^\dagger_{k_1\downarrow}c_{k_4\downarrow}: + \delta_{k_1,k_4}\theta(\varepsilon_{0\downarrow}-\varepsilon_1). \tag{A4b}$$

Inserting these expressions into Eq. (A3) yields, up to a constant term, $H_2 = H_\alpha + H_\phi$, with

$$H_\alpha = \frac{J^2\nu_0}{8}\sum_{\sigma,k_1,k_2}\sigma\ln\left[\frac{D}{B-B_0+\sigma(\varepsilon_1-\varepsilon_{0\sigma})}\right]c^\dagger_{k_1\sigma}c_{k_2\sigma} + \text{H.c.}, \tag{A5}$$

$$H_\phi = \frac{J^2}{8}\sum_{\{k_i\}}\frac{:c^\dagger_{k_3\uparrow}c_{k_2\uparrow}c^\dagger_{k_1\downarrow}c_{k_4\downarrow}:}{B-B_0+(\varepsilon_3-\varepsilon_{0\uparrow})-(\varepsilon_4-\varepsilon_{0\downarrow})} + \text{H.c.}, \tag{A6}$$

where D is the high-energy cutoff of the Kondo model. H_α describes elastic potential scattering. It can be expanded by assuming $(\varepsilon_{1,2}-\varepsilon_{0\sigma}) \ll B - B_0$. The zeroth order gives the first logarithmic correction to the zero-energy phase shifts,

$$\begin{Bmatrix}\delta_{0\uparrow}\\ \delta_{0\downarrow}\end{Bmatrix} = \begin{Bmatrix}\pi\\ 0\end{Bmatrix} \mp \frac{\pi\nu_0 J}{4} \mp \frac{\pi(\nu_0 J)^2}{4}\ln\left(\frac{D}{B-B_0}\right). \tag{A7}$$

Changing from wave vector to energy summations, the first and second orders obtained from Eq. (A5) reproduce precisely [87] H_α in Eq. (3), with $\bar\alpha_1 = 0$, $\alpha_2 = 0$ and

$$\frac{\alpha_1}{\pi} = \frac{(\nu_0 J)^2}{4(B-B_0)},\qquad \frac{\overline{\alpha}_2}{\pi} = -\frac{(\nu_0 J)^2}{8(B-B_0)^2}. \tag{A8}$$

Next, expand H_ϕ to first order in $(\varepsilon_{3,4}-\varepsilon_{0\sigma})/(B-B_0)$. The result coincides with H_ϕ in Eq. (3), with $\phi_2 = 0$,

$$\frac{\phi_1}{\pi} = \frac{(\nu_0 J)^2}{4(B-B_0)},\qquad \frac{\overline{\phi}_2}{\pi} = -\frac{(\nu_0 J)^2}{2(B-B_0)^2}. \tag{A9}$$

Equations (A7) to (A9) are the main results of this appendix. They explicitly give all the FL parameters in terms of the bare parameters of the Kondo model and the dummy reference energies $\varepsilon_{0\sigma} = -\frac{1}{2}\sigma B_0$, illustrating explicitly that the latter occur only in the combination $B - B_0$ [cf. Eq. (5)]. It is easy to verify explicitly that Eqs. (A7) to (A9) satisfy the FL relations (9) (in the latter, all derivatives w.r.t. ε_d vanish in the Kondo limit). Moreover, the above derivation clarifies the underlying reason for why the FL parameters necessarily must be mutually interrelated: they arise as expansion coefficients of the actual physical Hamiltonian in the large-field Kondo limit, namely H_2 of Eq. (A3), whose functional form fully fixes all terms in the expansion $H_2 = H_\alpha + H_\phi + \ldots$.

Equations (A7) to (A9) can also be used to test our predictions (17) for how the FL parameters are related to susceptibilities. To this end, we remove the dependence on the dummy reference energy by setting it to $\varepsilon_{0\sigma} = \mu_{0\sigma} = 0$ [as done in Eq. (11)]. Then, we directly compute the magnetization and spin susceptibility at large magnetic field. The Bethe ansatz solution provides a universal expression for the magnetization of the Kondo model,

$$m_d = \frac{1}{2} - \frac{1}{2\pi^{3/2}} \int_0^\infty dt\, \frac{\sin(\pi t)(\beta_r t)^{-t}}{t} \Gamma\left(\frac{1}{2}+t\right), \quad \text{(A10)}$$

where the ratio $\beta_r = \frac{\pi}{8}(B/T_K)^2 \geqslant \frac{1}{e}$ is written in terms of the Kondo temperature T_K extracted from the zero-field spin susceptibility [Eq. (20)]. At large magnetic fields, Eq. (A10) can be expanded in powers of $1/\ln \beta_r$. Noting that (we use that $T_K \sim D\, e^{-1/\nu_0 J}$)

$$\frac{2}{\ln \beta_r} \simeq \frac{\nu_0 J}{1+\nu_0 J \ln(B/D)} \simeq \nu_0 J + \dots, \quad \text{(A11)}$$

we also find an expansion for $\nu_0 J \ll 1$. At large magnetic fields, one obtains

$$m_d = \frac{1}{2} - \frac{\nu_0 J}{4}, \quad \chi_s = \frac{(\nu_0 J)^2}{4B}, \quad \frac{\partial \chi_s}{\partial B} = -\frac{(\nu_0 J)^2}{4B^2}. \quad \text{(A12)}$$

Inserting these susceptibilities into Eq. (17) for the FL parameters, we recover Eqs. (A8), (A9), which serves as a nice consistency check for Eq. (17). [Eq. (A12) for m_d does not strictly approach $\frac{1}{2}$ in the limit $B \to \infty$, because the calculation is perturbative in $\nu_0 J$]. In summary, in this appendix we explicitly derived the FL Hamiltonian at large magnetic field and checked the FL relations advertised in this paper.

APPENDIX B: RPT-FL DICTIONARY

It is instructive to relate the FL parameters introduced in this work to the parameters that are used in renormalized perturbation theory (RPT) [30,40–42,44] to parametrize the low-energy behavior of the retarded local Green's function of the impurity, $G_{d\sigma}(\omega) = 1/[\omega - \Sigma_\sigma(\omega)]$. If ω, T, and eV are so small that the impurity self-energy may be expanded to second order in these variables, this correlator can be expressed in the form

$$G_{d\sigma}(\omega) = \frac{\tilde{z}_\sigma}{\omega - \tilde{\varepsilon}_{d\sigma} + i\tilde{\Delta}_\sigma + \tilde{R}_\sigma + i\tilde{I}_\sigma}. \quad \text{(B1)}$$

All parameters carrying tildes are understood to be functions of magnetic field. $\tilde{z}_\sigma = [1 - \partial_\omega \Sigma'_\sigma(0)]^{-1}$ is the quasiparticle weight, $\tilde{\varepsilon}_{d\sigma} = [\varepsilon_{d\sigma} + \Sigma_\sigma(0)]\tilde{z}_\sigma$ the renormalized position of the local level with spin σ, and $\tilde{\Delta}_\sigma = \tilde{z}_\sigma \Delta$ its renormalized width. $\tilde{R}_\sigma$ and $\tilde{I}_\sigma$ are the real and imaginary parts of $-\Sigma^{(2)}_\sigma \tilde{z}_\sigma$, coming from the second-order term in the self-energy, which we parametrize as

$$\tilde{R}_\sigma = \tilde{R}_{\omega\sigma}\omega^2 + \tilde{R}_{V\sigma}\left[\tfrac{1}{3}(\pi T)^2 + \tfrac{1}{4}(eV)^2\right], \quad \text{(B2a)}$$

$$\tilde{I}_\sigma = \tilde{I}_{\omega\sigma}\left[\tfrac{1}{3}\omega^2 + \tfrac{1}{3}(\pi T)^2 + \tfrac{1}{4}(eV)^2\right], \quad \text{(B2b)}$$

where $\tilde{R}_{\omega\sigma}$, $\tilde{R}_{V\sigma}$, and $\tilde{I}_{\omega\sigma}$ are constants independent of ω, T, and eV. The imaginary part of the second-order self-energy can only depend on the combination of energy, temperature and bias stated in Eq. (B2b), because it is governed by the second-order term of the inelastic T matrix, which we know to depend only on this combination [Eq. (24b)]. The corresponding real part, however, requires two separate coefficients for its energy dependence and its temperature and voltage dependence [Eq. (B2a)], because the former also receives a contribution from the elastic T matrix, but the latter does not.

The spin-resolved version of the FL spectral function discussed in the main text is normalized such that $A_\sigma(0) = 1$ for the symmetric Anderson model at $T = V = B = 0$. It is related to the imaginary part of the local Green's function by $A_\sigma(\omega) = -(\pi\Delta)\frac{1}{\pi}\mathrm{Im}G_\sigma(\omega)$, hence [from Eq. (B1)]:

$$A_\sigma(\omega) = \frac{\tilde{\Delta}_\sigma(\tilde{\Delta}_\sigma + \tilde{I}_\sigma)}{(\omega - \tilde{\varepsilon}_{d\sigma} + \tilde{R}_\sigma)^2 + (\tilde{\Delta}_\sigma + \tilde{I}_\sigma)^2}. \quad \text{(B3)}$$

When this expression is expanded in the form of the spin-resolved versions of Eq. (26),

$$A_\sigma(\omega) = A_{0\sigma} + A_{1\sigma}\omega - \widetilde{C}_{A\sigma}\left[\tfrac{1}{3}(\pi T)^2 + \tfrac{1}{4}(eV)^2\right] - C_{A\sigma}\omega^2, \quad \text{(B4)}$$

and the expansion coefficients are expressed in terms of

$$\tilde{\rho}_\sigma = -\frac{1}{\pi}\mathrm{Im}G_{d\sigma}(0) = \frac{\tilde{\Delta}_\sigma/\pi}{\tilde{\Delta}_\sigma^2 + \tilde{\varepsilon}_{d\sigma}^2}, \quad \text{(B5)}$$

$$\sin(\delta_{0\sigma}) = \frac{\tilde{\Delta}_\sigma}{\sqrt{\tilde{\Delta}_\sigma^2 + \tilde{\varepsilon}_{d\sigma}^2}}, \quad \cos(\delta_{0\sigma}) = \frac{\tilde{\varepsilon}_{d\sigma}}{\sqrt{\tilde{\Delta}_\sigma^2 + \tilde{\varepsilon}_{d\sigma}^2}}, \quad \text{(B6)}$$

one readily obtains

$$A_{0\sigma} = \sin^2(\delta_{0\sigma}), \quad \text{(B7a)}$$

$$A_{1\sigma} = \pi\tilde{\rho}_\sigma \sin(2\delta_{0\sigma}), \quad \text{(B7b)}$$

$$\widetilde{C}_{A\sigma} = -\pi\tilde{\rho}_\sigma[\tilde{R}_{V\sigma}\sin(2\delta_{0\sigma}) + \tilde{I}_{\omega\sigma}\cos(2\delta_{0\sigma})], \quad \text{(B7c)}$$

$$\begin{aligned} C_{A\sigma} &= -\pi\tilde{\rho}_\sigma\left[\tilde{R}_{\omega\sigma}\sin(2\delta_{0\sigma}) + \tfrac{1}{3}\tilde{I}_{\omega\sigma}\cos(2\delta_{0\sigma})\right] \\ &\quad + (\pi\tilde{\rho}_\sigma)^2[4\sin^2(\delta_{0\sigma}) - 3]. \end{aligned} \quad \text{(B7d)}$$

By comparing Eq. (B7) to the expressions (27) of the main text, we can express all the FL parameters in terms of RPT parameters. Eqs. (B7b) and (B7c) imply

$$\alpha_{1\sigma} = \pi\tilde{\rho}_\sigma, \quad \phi_1 = \sqrt{\tfrac{2}{3}\pi\tilde{\rho}_\sigma\tilde{I}_{\omega\sigma}}, \quad \phi_{2\sigma} = -4\pi\tilde{\rho}_\sigma\tilde{R}_{V\sigma}. \quad \text{(B8a)}$$

Inserting these into Eq. (27c) and solving for $\alpha_{2\sigma}$, we find

$$\alpha_{2\sigma} = (\pi\tilde{\rho}_\sigma)^2\cot(\delta_{0\sigma}) + \pi\tilde{\rho}_\sigma\tilde{R}_{\omega\sigma}. \quad \text{(B8b)}$$

Equations (B8) constitute a useful dictionary that relates the RPT parameters, which characterize the impurity dynamics, to the FL parameters, which characterize the quasiparticle dynamics.

In conjunction with Eq. (13), the RPT-FL dictionary can be used to express the RPT parameters in terms of local ground-state susceptibilities; they can thus be computed exactly via the Bethe ansatz. Moreover, if alternative strategies (e.g. NRG) are used to compute the RPT parameters, then the relations (15) to (18) between various FL parameters that hold for certain special cases (zero field, or particle-hole symmetry, or the Kondo limit), suitably transcribed using the RPT-FL dictionary, provide useful consistency checks on the RPT parameters.

APPENDIX C: PERTURBATION RESULTS IN THE $\varepsilon_d \gg \Delta$ LIMIT

The FL coefficients needed to derive the spectral coefficients $\tilde{c}_A, c_A$ and transport coefficients c_V, c_T, depend on the zero-temperature dot occupation functions $n_{d\sigma}$ and their derivatives with respect to the level energy ε_d and magnetic field B. Deep in the empty-orbital regime, where $\varepsilon_d \gg \Delta$, the leading corrections to the noninteracting occupations,

$$n^0_{d\uparrow} = \tfrac{1}{2} - \tfrac{1}{\pi}\arctan\left[\left(\varepsilon_d - \tfrac{1}{2}B\right)/\Delta\right], \tag{C1}$$

can be computed perturbatively in the dot-lead hybridization, using the spin-down state of the dot as intermediate state (see also Ref. [86]), with the result

$$n_{d\uparrow} = n^0_{d\uparrow} - \frac{\Delta}{\pi}\frac{U n^0_{d\uparrow}\left(1 - n^0_{d\uparrow}\right)}{\left(U + \varepsilon_d + \frac{1}{2}B\right)\left(\varepsilon_d + \frac{1}{2}B\right)}, \tag{C2a}$$

$$n_{d\downarrow} = \frac{\Delta}{\pi}\left(\frac{1 - n^0_{d\uparrow}}{\varepsilon_d + \frac{1}{2}B} + \frac{n^0_{d\uparrow}}{\varepsilon_d + U + \frac{1}{2}B}\right). \tag{C2b}$$

All FL parameters can be straightforwardly computed from these expressions using Eqs. (12) and (13). To compare with the numerical results in Fig. 7, we substitute $\varepsilon_d \to \tilde{\varepsilon}_d$ [cf. Eq. (42)] in the final result for c_V.

[1] D. Goldhaber-Gordon, H. Shtrikman, D. Mahalu, D. Abusch-Magder, U. Meirav, and M. Kastner, Nature (London) **391**, 156 (1998).
[2] A. Kogan, S. Amasha, D. Goldhaber-Gordon, G. Granger, M. A. Kastner, and H. Shtrikman, Phys. Rev. Lett. **93**, 166602 (2004).
[3] A. A. Houck, J. Labaziewicz, E. K. Chan, J. A. Folk, and I. L. Chuang, Nano Lett. **5**, 1685 (2005).
[4] S. Amasha, I. J. Gelfand, M. A. Kastner, and A. Kogan, Phys. Rev. B **72**, 045308 (2005).
[5] C. H. L. Quay, J. Cumings, S. J. Gamble, R. dePicciotto, H. Kataura, and D. Goldhaber-Gordon, Phys. Rev. B **76**, 245311 (2007).
[6] T. S. Jespersen, M. Aagesen, C. Sørensen, P. E. Lindelof, and J. Nygård, Phys. Rev. B **74**, 233304 (2006).
[7] T.-M. Liu, B. Hemingway, A. Kogan, S. Herbert, and M. Melloch, Phys. Rev. Lett. **103**, 026803 (2009).
[8] L. Glazman and M. Raikh, Pis'ma Zh. Eksp. Teor. Fiz. **47**, 378 (1988) [JETP Lett. **47**, 452 (1988)].
[9] T. K. Ng and P. A. Lee, Phys. Rev. Lett. **61**, 1768 (1988).
[10] L. Glazman and M. Pustilnik, in *New Directions in Mesoscopic Physics (Towards Nanoscience)*, edited by R. Fazio, V. Gantmakher, and Y. Imry (Kluwer, Dordrecht, 2003); M. Pustilnik and L. Glazman, J. Phys.: Condens. Matter **16**, R513 (2004).
[11] A. M. Chang and J. C. Chen, Rep. Prog. Phys. **72**, 096501 (2009).
[12] A. Rosch, J. Paaske, J. Kroha, and P. Wölfle, Phys. Rev. Lett. **90**, 076804 (2003).
[13] S. Kehrein, Phys. Rev. Lett. **95**, 056602 (2005).
[14] B. Doyon and N. Andrei, Phys. Rev. B **73**, 245326 (2006).
[15] L. G. G. V. Dias da Silva, F. Heidrich-Meisner, A. E. Feiguin, C. A. Busser, G. B. Martins, E. V. Anda, and E. Dagotto, Phys. Rev. B **78**, 195317 (2008).
[16] H. Schoeller, The European Physical Journal Special Topics **168**, 179 (2009).
[17] J. Eckel, F. Heidrich-Meisner, S. Jakobs, M. Thorwart, M. Pletyukhov, and R. Egger, New J. Phys. **12**, 043042 (2010).
[18] C. P. Moca, P. Simon, C. H. Chung, and G. Zaránd, Phys. Rev. B **83**, 201303 (2011).
[19] R. Gezzi, T. Pruschke, and V. Meden, Phys. Rev. B **75**, 045324 (2007).
[20] W. Metzner, M. Salmhofer, C. Honerkamp, V. Meden, and K. Schönhammer, Rev. Mod. Phys. **84**, 299 (2012).
[21] M. Pletyukhov and H. Schoeller, Phys. Rev. Lett. **108**, 260601 (2012).
[22] S. Smirnov and M. Grifoni, Phys. Rev. B **87**, 121302 (2013).
[23] A. Schiller and S. Hershfield, Phys. Rev. B **58**, 14978 (1998).
[24] E. Boulat and H. Saleur, Phys. Rev. B **77**, 033409 (2008).
[25] F. B. Anders and A. Schiller, Phys. Rev. Lett. **95**, 196801 (2005).
[26] F. B. Anders, Phys. Rev. Lett. **101**, 066804 (2008).
[27] G. Cohen, E. Gull, D. R. Reichman, and A. J. Millis, Phys. Rev. Lett. **112**, 146802 (2014).
[28] A. Dorda, M. Ganahl, H. G. Evertz, W. von der Linden, and E. Arrigoni, Phys. Rev. B **92**, 125145 (2015).
[29] An attempt in this direction was made in Ref. [30] for the symmetric Anderson model, using renormalized perturbation theory. However, their results disagree with the results presented here (see the end of Sec. III C).
[30] A. C. Hewson, J. Bauer, and A. Oguri, J. Phys.: Condens. Matter **17**, 5413 (2005).
[31] A. Rosch, J. Paaske, J. Kroha, and P. Wölfle, J. Phys. Soc. Jpn. **74**, 118 (2005).
[32] P. Nozières, J. Low Temp. Phys. **17**, 31 (1974); in *Proceedings of the 14th International Conference on Low Temperature Physics*, Vol. 5, edited by M. Krasius and M. Vuorio (North Holland, Amsterdam, 1974), p. 339–374; P. Nozières, J. Phys. **39**, 1117 (1978).
[33] K. Yosida and K. Yamada, Prog. Theor. Phys. **46**, 244 (1970); K. Yamada, *ibid.* **53**, 970 (1975); K. Yosida and K. Yamada, *ibid.* **53**, 1286 (1975); K. Yamada, *ibid.* **54**, 316 (1975).
[34] A. Yoshimori, Prog. Theor. Phys. **55**, 67 (1976).
[35] L. Mihály and A. Zawadowski, J. Phys. (Paris), Lett. **39**, 483 (1978).
[36] R. Sakano, T. Fujii, and A. Oguri, Phys. Rev. B **83**, 075440 (2011).
[37] R. Sakano, A. Oguri, T. Kato, and S. Tarucha, Phys. Rev. B **83**, 241301 (2011).
[38] C. B. M. Hörig, C. Mora, and D. Schuricht, Phys. Rev. B **89**, 165411 (2014).
[39] M. Hanl, A. Weichselbaum, J. von Delft, and M. Kiselev, Phys. Rev. B **89**, 195131 (2014).

[40] A. C. Hewson, *The Kondo Problem to Heavy Fermions* (Cambridge University Press, Cambridge, 1993).
[41] A. C. Hewson, J. Phys. Soc. Jpn. **74**, 8 (2005).
[42] A. C. Hewson, Phys. Rev. Lett. **70**, 4007 (1993); J. Phys.: Condens. Matter **5**, 6277 (1993); Adv. Phys. **43**, 543 (1994); J. Phys.: Condens. Matter **13**, 10011 (2001); A. C. Hewson, A. Oguri, and D. Meyer, Eur. Phys. J. B **40**, 177 (2004); A. C. Hewson, J. Bauer, and W. Koller, Phys. Rev. B **73**, 045117 (2006); J. Bauer and A. C. Hewson, *ibid.* **76**, 035119 (2007); K. Edwards and A. C. Hewson, J. Phys.: Condens. Matter **23**, 045601 (2011); K. Edwards, A. C. Hewson, and V. Pandis, Phys. Rev. B **87**, 165128 (2013); V. Pandis and A. C. Hewson, *ibid.* **92**, 115131 (2015).
[43] I. J. Hamad, C. Gazza, J. A. Andrade, A. A. Aligia, P. S. Cornaglia, and P. Roura-Bas, Phys. Rev. B **92**, 195113 (2015).
[44] A. C. Hewson, J. Phys.: Condens. Matter **18**, 1815 (2006).
[45] F. Lesage and H. Saleur, Phys. Rev. Lett. **82**, 4540 (1999); Nucl. Phys. B **546**, 585 (1999).
[46] L. Freton and E. Boulat, Phys. Rev. Lett. **112**, 216802 (2014).
[47] C. Mora, C. P. Moca, J. von Delft, and G. Zaránd, Phys. Rev. B **92**, 075120 (2015).
[48] A. Oguri, Phys. Rev. B **64**, 153305 (2001).
[49] L. Glazman and M. Pustilnik, in *Nanophysics: Coherence and Transport*, edited by H. Bouchiat (Elsevier, Amsterdam, 2005), pp. 427–478 .
[50] E. Sela, Y. Oreg, F. von Oppen, and J. Koch, Phys. Rev. Lett. **97**, 086601 (2006).
[51] A. Golub, Phys. Rev. B **73**, 233310 (2006).
[52] A. O. Gogolin and A. Komnik, Phys. Rev. Lett. **97**, 016602 (2006).
[53] C. Mora, X. Leyronas, and N. Regnault, Phys. Rev. Lett. **100**, 036604 (2008).
[54] C. Mora, Phys. Rev. B **80**, 125304 (2009).
[55] C. Mora, P. Vitushinsky, X. Leyronas, A. A. Clerk, and K. Le Hur, Phys. Rev. B **80**, 155322 (2009).
[56] P. Vitushinsky, A. A. Clerk, and K. Le Hur, Phys. Rev. Lett. **100**, 036603 (2008).
[57] T. Fujii, J. Phys. Soc. Jpn. **79**, 044714 (2010).
[58] K. G. Wilson, Rev. Mod. Phys. **47**, 773 (1975).
[59] R. Bulla, T. A. Costi, and T. Pruschke, Rev. Mod. Phys. **80**, 395 (2008).
[60] A. Weichselbaum, Phys. Rev. B **86**, 245124 (2012).
[61] M. Garst, P. Wölfle, L. Borda, J. von Delft, and L. Glazman, Phys. Rev. B **72**, 205125 (2005).
[62] In the nonuniversal case of a finite bandwidth, the Fermi liquid relations that we derive are no longer strictly valid. Nevertheless, the corrections to our predictions are expected to be small with the ratio of the maximum of Δ, B, $|\varepsilon_d|$, and U over the bandwidth of the model.
[63] I. Affleck and A. W. W. Ludwig, Nucl. Phys. B **360**, 641 (1991).
[64] I. Affleck and A. W. W. Ludwig, Phys. Rev. B **48**, 7297 (1993); A. Tsvelick and P. Wiegmann, Adv. Phys. **32**, 453 (1983).
[65] See Supplemental Material at http://link.aps.org/supplemental/10.1103/PhysRevB.95.165404, where the Bethe ansatz expressions used here are reviewed.
[66] F. D. M. Haldane, Phys. Rev. Lett. **40**, 416 (1978).
[67] F. D. M. Haldane, J. Phys. C **11**, 5015 (1978).
[68] Y. Meir and N. S. Wingreen, Phys. Rev. Lett. **68**, 2512 (1992).
[69] Y. M. Blanter and M. Büttiker, Phys. Rep. **336**, 1 (2000).
[70] A. Kamenev and A. Levchenko, Adv. Phys. **58**, 197 (2009).
[71] Expression (24b) for $\mathcal{T}_\sigma^{\rm inel}$ stems from the quadratic contribution of the ϕ_1 term in H_ϕ to the quasiparticle self-energy. Its $\varepsilon^2 + (\pi T)^2$ contribution is well known in an equilibrium context [32,64]. We obtained its $(eV)^2$ contribution as follows. Since ε^2, T^2, and $(eV)^2$ all characterize the phase space available for inelastically scattering a quasiparticle having energy ε, their contributions all have the same general form, differing only by numerical prefactors. We deduced that of $(eV)^2$ to be $\frac{3}{4}$ by inserting a general low-energy expansion for $A(\varepsilon)$ into (23) for $G(T,V)$, expanding the latter in the form (29) and equating the resulting expression for C_V to the quantity c_V/E_*^2 found in Ref. [47] by a direct calculation of the current. The resulting combination $[\varepsilon^2 + (\pi T)^2 + \frac{3}{4}(eV)^2]$ in Eq. (24b) for $\mathcal{T}_\sigma^{\rm inel}(\varepsilon)$ is consistent with that reported in Eq. (43) of Ref. [88] for the imaginary part of the local self-energy in renormalized perturbation theory.
[72] The numerical prefactor for $\widetilde{C}_A$ was chosen to ensure that $\widetilde{C}_A = C_A$ in the Kondo limit at zero field, see Eq. (34a).
[73] A. A. Aligia, J. Phys.: Condens. Matter **24**, 015306 (2012).
[74] E. Muñoz, C. J. Bolech, and S. Kirchner, Phys. Rev. Lett. **110**, 016601 (2013).
[75] A. A. Aligia, Phys. Rev. B **89**, 125405 (2014).
[76] T. A. Costi, Phys. Rev. Lett. **85**, 1504 (2000).
[77] C. J. Wright, M. R. Galpin, and D. E. Logan, Phys. Rev. B **84**, 115308 (2011).
[78] R. Zitko, R. Peters, and T. Pruschke, New J. Phys. **11**, 053003 (2009).
[79] J. E. Moore and X.-G. Wen, Phys. Rev. Lett. **85**, 1722 (2000).
[80] A. Weichselbaum, F. Verstraete, U. Schollwöck, J. I. Cirac, and J. von Delft, Phys. Rev. B **80**, 165117 (2009).
[81] We computed discrete NRG data for the spectral function using the full-density-matrix NRG of Ref. [89]. (NRG details: we used a discretization parameter of $\Lambda = 2$, kept 1024 states, did not do any z averaging and did not employ the so-called self-energy trick). We extracted $\tilde{C}_A$ and C_A from discrete NRG data by employing the procedure described in Sec. IV C of Ref. [39] to compute the coefficients a_0 and a_2 of Eq. (42) there, using $\tau = 0.7$ for the broadening parameter introduced in Eq. (45) there.
[82] A. C. Hewson (private communication).
[83] P. Wiegmann, Phys. Lett. A **80**, 163 (1980); N. Kawakami and A. Okiji, J. Phys. Soc. Jpn. **51**, 2043 (1982); P. Wiegmann and A. Tsvelick, J. Phys. C **16**, 2281 (1983); A. Tsvelick and P. Wiegmann, *ibid.* **16**, 2321 (1983).
[84] H. Grabert and M. H. Devoret, *Single Charge Tunneling: Coulomb Blockade Phenomena in Nanostructures* (Springer Science & Business Media, New York, 2013), Vol. 294.
[85] Equation (42) is derived from the seminal expression of the renormalized level provided by Haldane in Ref. [66], $\varepsilon_d^* = \varepsilon_d + \frac{\Delta}{\pi} \ln \frac{W_0}{W}$, in which W_0 is the energy scale at which the orbital energy renormalization starts, namely, $W_0 \sim \varepsilon_d + U$, and W the energy scale in which the renormalization stops, i.e., $W \sim \alpha\varepsilon_d$. Notice that this formula for ε_d^* applies within a regime different from the mixed valence regime; in the latter, $|\varepsilon_d| < \Delta$, hence ε_d is the lowest energy scale in the problem and the renormalization

stops at $\Delta \ll U$. For the data sets presented in Fig. 7(a), ε_d is still comparable to (but somewhat larger than) the hybridization energy Δ and the charging energy U.

[86] M. Filippone, K. Le Hur, and C. Mora, Phys. Rev. B **88**, 045302 (2013).

[87] up to terms which can be written as total derivatives in the action formalism, see Supplementary note S-IV in Ref. [47].

[88] A. Oguri, J. Phys. Soc. Jpn. **74**, 110 (2005).

[89] A. Weichselbaum and J. von Delft, Phys. Rev. Lett. **99**, 076402 (2007).